Dear recommender,
First we wanted to thanks you and the two reviewers for their impressive work, questions and suggestions. They allowed us to modify the paper in order to improve its structure. Especially, we split the section 'Results and discussion' into to two separate parts. Moreover, we deeply rewrote the whole discussion part, trying to make it easier to read. In parallel, few figures have been modified in order to improve their analyse.
We also answered all the questions, either in the paper or in this document. We provide here a new version of the paper. As additional data, we also joined a commented version of the paper, with all changes, making easier the tracking of changes. We hope that all the modifications provided here make the paper easier to read and that it becomes now suitable for recommendation by PCI.
Sincerely yours
Arnoul Van Rooij and co-authors

E. dreyer (recommender):

An interesting manuscript on the biomechanics of branch growth in trees that requires however a careful revision

This interesting manuscript proposing a modelling approach to the question of the biomechanics of a growing branch has been analysed by two specialists of biomechanics (which, as a recommender, I am not).

The two external reviewers provided a detailed analysis of the manuscript (see their comments below or in the attached document). I had a look at the general structure and the logic of the manuscript too, and provided some detailed comments and suggestions as annotations in the attached version of the manuscript.

The external reviewers found the model quite interesting and novel with respect to the existing literature on this very specialised topic in tree biology. They in general agree with the approach used to quantify two components of the structure of a growing branch: the eccentricity and the production of reaction wood. They found the model to be in general clearly described and based on a number of clear analytical equations. One of the reviewers however wondered why allometric relationships were used as entry to the model, and this concern needs be addressed. The model is then tested against a small set of data combining a branch from a large pine tree (taken as an example of a softwood conifer tree) and a cherry tree (taken as an example of a hardwood tree). This test of optimality is very interesting. However, one of the reviewers was concerned by the fact that the procedure used to test the optimality of a given growth strategy needed to be made more explicit. This should be done with some details at the end of the introduction, when the experimental procedure (combining modelling and test) is described in more details; by the way, I found that the current description lacks some details about the rationale and the demonstration to be made.

We answer to the reviewer on this concern (see below). We formalize what we call 'optimal' and we tried to make the part on the allometric law clearer.

There are also concerns about the structure and organisation of the manuscript. One of the referees stated that the manuscript sounded like having been written in several steps, with changes in the wording of the concepts used; I had the same feeling. Furthermore, my suggestion would be to clearly separate the presentation of the results from the discussion: such a clear distinction leads to the presentation of the results in a short manner, and a more structure discussion that can in places cover more than just putting the results into perspective.

We changed the structure by splitting "results and discussion" in two separate parts. Also, we worked on the whole manuscript in order to remove the feeling of the "several step writing". Especially, we removed the the redundancies and have been careful to use the same wording all along the article.

A concept that requires a better definition and a more consistent use is that of "growth strategy": here, it is used in the sense of the relative contribution of two different processes: eccentricity (accumulation of wood on one side of the branch to counteract the effects of gravity) and the formation of reaction wood (accumulation of tension wood in softwood trees (angiosperms) and compression wood in conifers (gymnosperms) that also counteracts the effects of gravity by changes in the ultrastructure of the wood tissues. The "strategy" is meant here as the balance between the two effects if I understood well the aims of the research. This needs be made clearer in the text. The same wording should then be used consistently across the manuscript.

Indeed, it seems that the term 'strategy' was not suitable to describe the situation. This wording refered to anthropomorphism concepts. Therefore, we deleted it and replaced with 'growth option' or 'growth parameter' the tree could use.

Finally, there is a need to make clear that the experimental basis of the manuscript does not allow to oppose gymnosperms and angiosperms as there is only one sample per category. I am sure the authors are perfectly aware of this, but some wording in the manuscript might give the wrong impression they are not. This was highlighted in the attached copy of the text.

Indeed, it was not clear. We have reworded it in this way.

To summarize, there is a consensus that the manuscripts will ultimately deserve a recommendation, but that there is a need to improve its structure and clarity before this positive recommendation might be issued by the Peer Community in Forest and Wood Sciences. The manuscript has the potential of becoming a very nice and important contribution in the field of tree biomechanics.

Erwin Dreyer, acting as recommender for this manuscript.

Anonymous review1:

The aim of this article is to explore which strategies minimize internal stresses during branch growth. The main hypothesis (which is verified later on Figure 12) is vertical bending moment prevails over the torsional moment, and horizontal bending moment. Based on this hypothesis the growth kinematic is simplified to specifically resist such vertical bending moment: the branch section remains circular during growth and the only degree of freedom is the position of the center of the circle along the vertical line coined eccentricity. A linear relationship between elastic strain, bending strain, radius increments, force and moment increments is derived from static force balance and Hooks law (12a,12b); the coefficients of the linear relationship are expressed as function of the two maturation stresses and the eccentricity. Force and moment are supposed to depend on the radius R following allometric laws whose coefficients are estimated through simulations of trees with AMAPsim (Figure 4, Table 1).
Equation 12a combined with the allometric laws for force and moments provides the elastic strain. Bending strain are also supposed to depend on the radius R following allometric relationships thus Equation 12b provides an equation between the two maturation stresses and the eccentricity (21a for hard wood and 21b for soft wood). Based on these allometric laws an analytic formula is provided for the stresses as a function of r (19). The two growth strategies derive from the fundamental equation (20), either supposing a constant eccentricity while the maturation stress difference (varying with r) drives the postural control or supposing a constant maturation stress difference while the eccentricity (varying with r) drives the postural control.

Once allometric law have been determined the model is fully analytical: For each strategies stresses are computed with formula (19) for increasing radius (the radius being the proxy for growth) as well as the driving variable (eccentricity or maturation stresses difference). The optimal strategy is the one which minimizes stresses at the periphery which are compressed to maximal stresses observed in the literature; stresses at the pith are not considered as they diverge due to an oversimplified model (discussed in the section Limits of the model). The strategies are compared for one hardwood species Prunus avium and one softwood species Pinus pinaster.

The article is interesting and globally well-written but I feel there were several phases of writing; the article is long and not completely coherent. I recommend publication once the following concerns are addressed: The model is clearly detailed and rigorous. In my eye, the main limitation is the use of allometric laws to complete equation 12a, 12b to get equation 19 and 21. I do not see why an allometric is used for b but not for a; I am not a specialist and I can't judge the robustness of such an hypothesis but from far away it appears as an adhoc simplification. It could be more quantitatively discussed (narrowness of the allometric distribution). Later on the growth is supposed to be stationary so the b does not depend on r except in the paragraph, « Influence of the orientation ... ». In this paragraph you should explain why for up-righting and passive bending curves you do not use allometric law fo bending strain but other driver (« increasing weight » or « maturation gradient »). The whole is a bit fuzzy for me.

Only two allometric laws are used in the model (equations 16.a and 16.b). These are hypothesis about the loading history of the branch, based on the fitting of AMAP data. There isn't any allometric law for the strain component a and b.
3 orientation scenarii are envisaged: 1. stationarity, meaning b=0, 2. up-righting and 3. passive bending. Both scenarios 2 and 3 depend on the interaction between increasing weight (therefore allometric laws 16) and maturation gradient (equation 9). Even if equation 18 looks like an allometric law, it is just a way to reformulate in a general way scenarios 2 and 3. However, we hope the new version we provide here is clearer for the reader. We worked for this!

I had more difficulties to follow the discussion which probably comes from the fact I am not a specialist. In my eyes, the criteria for optimality of a strategy are not sufficiently explained: Is it solely the stress at the periphery?

An optimal stress pattern is the one that generates the lowest elastic energy stored in the section. As our Young's modulus is spatially homogenous, this means that the optimal stress pattern minimizes both tensile stress at periphery and compression stress in the pith. In a real situation, there may be plastic deformation in the pith, limiting compressive stress, and leading to more tension on periphery. In our case, we could compute the variance of the integrated stress to get a criteria of optimality, but we chose to just look at 1./ The tension a periphery and 2./ The area where compressive stress was high.

Is there a cost when eccentricity or maturation stress are too high?

The ultimate theoretical cost is the fracture of the branch. It could be caused by a maturation stress level higher than the failure stress, or an eccentricity leading to a pattern with high stress level too. Before cracks pattern appears, the branch probably could not support its own weight anymore; leading to a bending downward. However, this scenario remains rare (either from literature or from our own observation).

For instance, I do not understand the following statement: « When combined, it seems more efficient to vary the eccentricity and keep a constant difference of maturation stress than to keep a uniform eccentricity and to vary the maturation stress. « When I look to figures 6.a.i and 6.b.i: maximal stress for the strategy beta=0 seems to rank as well as for e=0.5.
This sentence was not really relevant. However, in the new improved version, the figures changed and the referring comments were modified.

The figures and legend could also be improved:
- The use of r for both figure 5b and 5c (and all the following figures 6,7,8,9) was confusing: I would use x for 5b and r for 5c.
- The legend should be more homogeneous Figure 5 « constant difference of maturation stress « , Figure 6 « constant maturation gradient ». It would more logical to represents sigmaNW-SigmaTW than beta in the legend.

Thank you for your suggestion. Figures has been changed taking into account your comments. “x” was used instead of “r”. Also, we changed “r” into “R” for figure 5.c and f (and the following). R is the radius of the cross section at the corresponding time t, while r is the radial polar coordinate. We modified the text accordingly. On Figure 5 and 7, the scale on the axis of the stress map 5.a (7.a) were modified in order to become more homogeneous with other graphs. Finally, we chose to replace the representation of the different section 5.d (7.d) by a stress map too. It makes the figure clearer and gives more information to the reader. Legends have been also improved:,we replaced “beta” by sigmaNW and RW. Also, caption has been rewritten. To illustrate our changes, please find bellow original figure 5 vs. the new one.

Old:

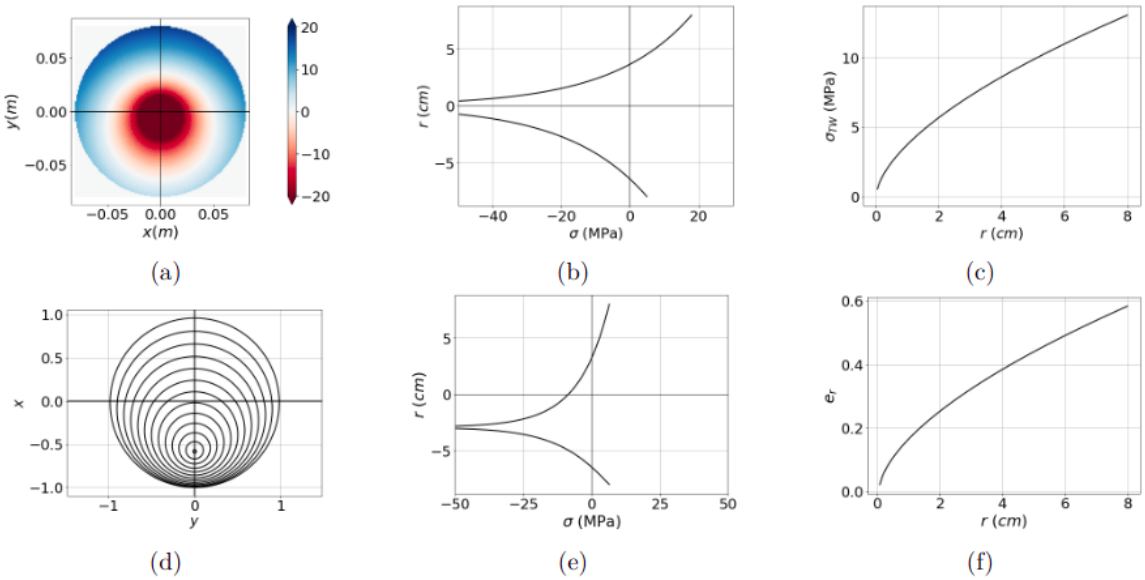

Figure 5: *Prunus avium*: Horizontal orientation maintained by the two different drivers: a-c) maturation stress and d-f) eccentricity. Different types of representation are proposed: a) (resp. d)) 2D visualisation of the growth stress (resp. eccentricity) in the whole section. b) and e) Growth stress profile on the line y=0. c) and f) Parametric representation of the tropic driver: maturation stress and eccentricity.

New:

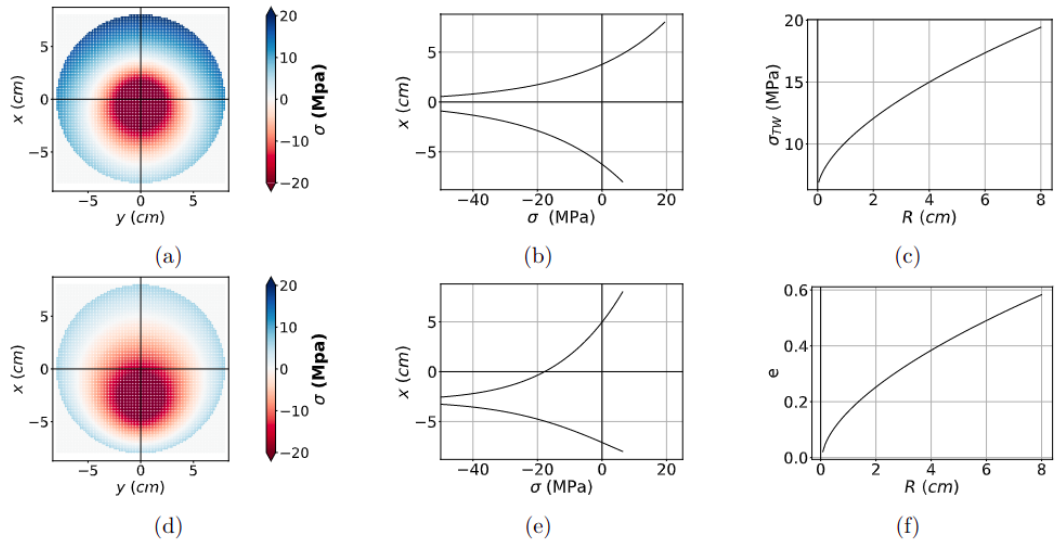

Figure 5: *Prunus avium*: The horizontal orientation of the branch is maintained by the two different processes: (a-c) the maturation stress provided by the formation of reaction wood; (d-f) the eccentric growth; (a,d) 2D visualisation of the growth stress in the whole section; (b,e) Growth stress profile on diameter y=0. (c,f) Parametric representation of the tropic driver, maturation stress (c) and eccentricity (f).

I do not understand “In case of combined effects, although eccentricity alone ensures stationarity, it does not succeed anymore when combined to a uniform maturation (red dotted line in Fig. 8.b). “ First there is no red dotted line on figure 8.
I thought “stationarity” was an hypothesis to suppose b independant of r which is at the basis of the model. How can you contradict an hypothesis of the model?

The review was right: our text was confusing in this part. When compression stress is too low, there is a coordination problem in our growth scenario: at the first stage of the development, the stress gradient tends to bend the branch upward, and the eccentricity has to balance this tendency, leading to high negative (and unrealistic) eccentricity. There is a limit compression stress which is lower than sigmaNW (red curve in the old graph), which is why there isn’t any red curve in the plot. In the new version, we updated the plot and the discussion to make it clearer.

Old Fig 8:

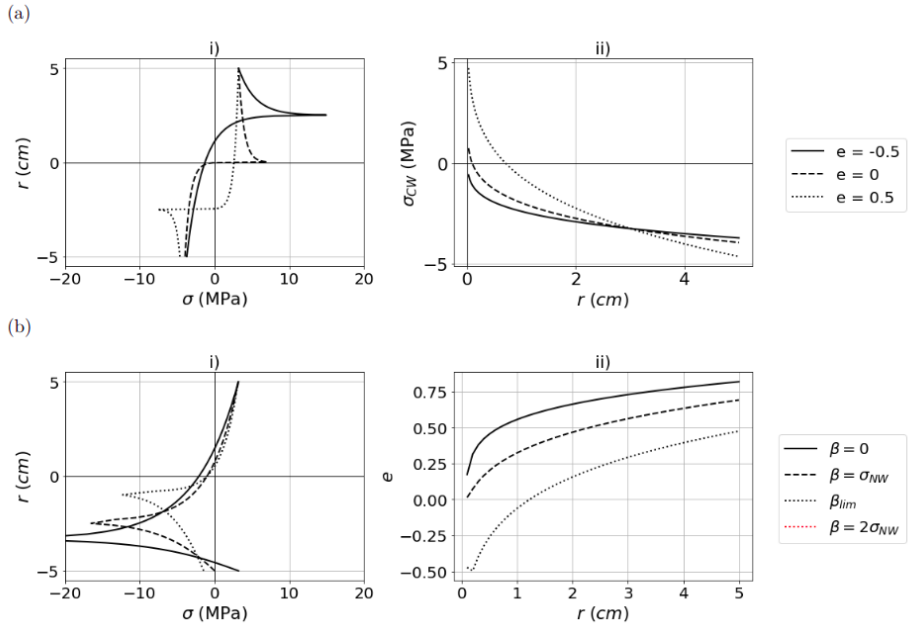

Figure 8: Illustration of different straightening strategies: (a) constant eccentricity, the maturation is the main driver of postural control; (b): constant maturation gradient, the eccentricity is the main driver of postural control.

New Fig 8:

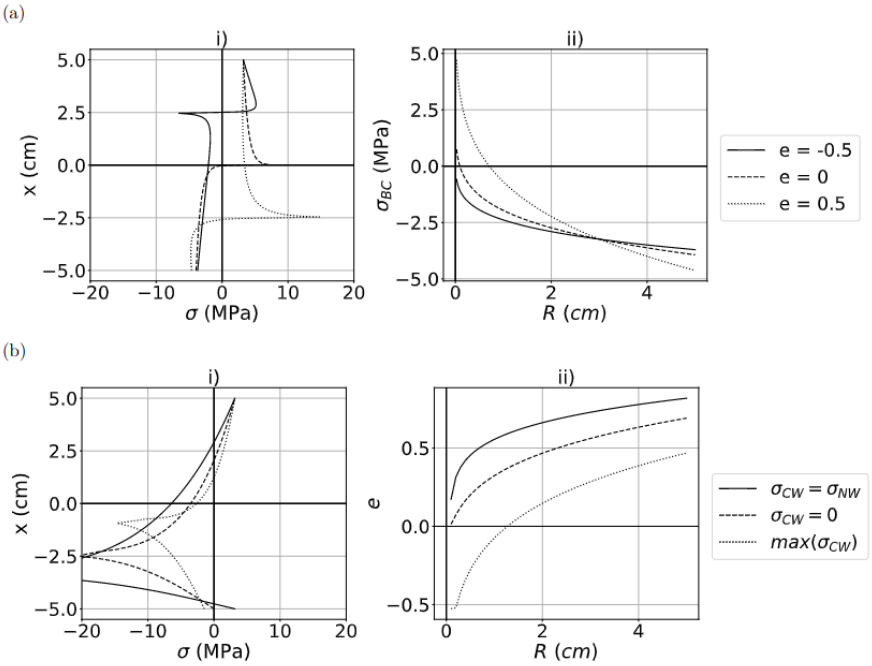

Figure 8: Different possible options to maintain the orientation of *Pinus pinaster* branches: (a) a constant eccentricity combined with the maturation that becomes the main driver of postural control; or (b) a constant maturation gradient combined with an eccentricity that becomes the main driver of postural control.

In general, the Results and discussion should be clarified and a bit more structured.

We completely re-edited the "discussion and results" part (now split into "results" and "discussion" sections), hopefully taking into account your comments. Moreover, we rewrote this part in order to make the analysis clearer and easier for the readers.

Reviewer 2:

Paper by Van Rooij et al. presents a revised biomechanical model simulating the growth stress distribution in a branch cross-section. The originality of the paper is application of the biomechanical model on outputs of a growth model generating the tree architecture and the growth history i.e. history of mechanical loading. Authors then play with two main parameters controlling the branch postural control: maturation stresses and eccentric growth.
The rationale of the paper is very interesting however, some clarifications in the used terminology and discussion of outputs should be done.

Results and conclusion section lacks comparison with literature and sometimes the link with possible biological interpretation.

Result and discussion have been completely rewritten, with more links with existing literature. Terminology has been changed taking into account your comments (see following remarks). Biological questions are set in terms of perspective.

Language revision would be appreciated.

We corrected many mistakes and other language defaults. We hope this new improved version is now suitable.

Title: growth strategies -> biomechanical strategies?

We agree that "strategy" was an inappropriate wording. We changed this in the entire manuscript and we suggest to replace "strategy" by "option" that does not refer to anthropomorphism concept but refers to the fact that trees have several physiological possibilities to respond to a constrain. We have changed and adapted the title accordingly In the text, we use now the expressions 'parameters', 'options' and 'lever'.

Abstract

L12 Ensure > control
L12 gravity -> its self-weight
Corrected

L12 I am not sure we can talk about different strategies while talking about maturation stress and eccentricity, I would rather talk about different parameters
Indeed, the term strategy was not fully relevant . See our comment in the previous section.

L13 I am a bit bothered by the term straightening. As you say later in your paper, the most straightforward assumption for the branch is to maintain its spatial position, not to search for a vertical position at it is the case of the main stem axis. By the way, straightening might by also confused with proprioception, which is not of concern here.
For us, straightening means to maintain the spatial position, and there is no confusion. However, to make it clearer, we chose to change it by some reformulations like 'posture maintenance', 'maintaining the posture', 'maintain of the orientation', 'orientation maintenance'. We hope these new expressions make are more suitable for the readers.

L16 ...biomechanical impact of each strategy, what do you mean?
The consequences of each option on the mechanical distribution of the longitudinal stress on the section. This sentence has not been reworded.

L20 Eccentricity process - I would rather talk about eccentric growth.
The reader is right. Actually, we now use "eccentric growth" and "eccentric radial growth"
L23 Biomechanical process? The term building does not seem appropriate to me for plants.
The reviewer is right. We changed this expression

Introduction

L28 construction of architecture, postural maintenance and resistance to external elements is not very clear, please reword
Corrected: see L28 *"construction of the tree architecture, postural control of trunk and branches and breaking resistance to external stimuli"*

L80 I think the first biomechanical difference between the stem and the branch is that the tree stem is looking for verticality, which is not the case of the branch as mentioned above. I think you should

introduce it here, explicit more clearly hypothesis you want to test with your model and also the final aim – why study the capacity of branches to control their posture is interesting.

We thank the reviewer for the suggestion. In the new version, the end of the introduction has been changed taking into account your comments (see the commented version attached to get more information). In particular, we added this paragraph on L84-91:

"*Unlike trunks, which usually seek verticality, after the first stages of growth, branches tend to grow in a stationary way at a fixed angle to the vertical. Therefore, in this framework, we focus on understanding of the motor processes driving the control of branch orientation, through the study of two growth parameters: eccentric radial growth and RW. The objective is to compute the mechanical efficiency of each biological option in order to evaluate if it is realistic and safe for the branch. For this purpose, we developed a semi-incremental biomechanical model of growth stress at the cross section level that takes into account the eccentricity and maturation gradients during the construction of branches. Using the digital models of one softwood Pinus pinaster and one hardwood Prunus avium, the impact of each of these two growth parameters on the stress state was evaluated.*"

Material and methods

L149 balances –> compensates
Done
L167 realistic data -> data generated by growth model
Done
L169 Tree architecture modelling
Done

L171 Could you explain reasons for the selection of these two species?

Our model needed realistc data. No experimental data were available. We collaborated with AMAP team that already computed realistic trees using experimental data coming from huge architectural data bases. Modelling one species requires a very long time for the AMAP team, and requires a huge amount of experimental data. Today, there is only few species available, and only two temperate species: the birch and the pine tree. Our model was only compatible with temperate architecture modelling (each new layer can be a year, or a uniform part of a year). This drove our choice.

AMAPSim is simulating open- grown trees or forest trees?

AMAPSim can simulate different situations, and both open-grown and forest trees. In this work, open-grown tree has been selected. We did not want to use any other dimensioning markers than the usual ones (gravity and light search). We added more information on this point in L179-181.

Birch trees are in general smaller and live shorter compared to Pinus pinaster, does the age of 50 years correspond roughly to the same stage of architectural development?
The comment of the reviewer is relevant. Our trees do not have the same ontological age. However, the main concern was to get mature trees, with branches old enough to have a significant loading history. After discussions with AMAP team members, we generated two mature trees with the same age. Even if the architectural development is not exactly at the same stage, there are two mature trees (see L181).

What is the height and diameter of simulated trees? What are dimensions (and its variability) of generated branches?

In the previous version, the information was scarce. In the new version, we added a section (L181-188) where we provide more information on both trees and tree branches. Concerning trees, the height, diameter at the base, and insertion height of the first branch is given. The geometrical distribution and variability (length, radius and insertion angle) of main branches are now also available in table 1 (L188)

L182: "*In the final state, the pine (resp. birch) was 18,2 m (resp. 14,1 m) high. The diameter at the base was 40 cm for both species. The insertion height of the first branch was 14,3 m for pine and 4,6 m for the birch. The branches of interest were the main branches; those that were directly attached to the trunk. In addition, only branches that were more than 20 years old have been studied, so that they had a consistent loading history. Finally, 33 branches for the pine and 45 for the birch were selected. For each of the branch groups, the distributions of length L, radius r and insertion angle with the trunk θ are shown in Table 1*

Species	L_m (m)	r_m (m)	θ_m (°)
Pinus pinae	5.3 ± 0.4	5.2 ± 0.3	70 ± 0.01
Prunus avium	7.9 ± 1.4	8.1 ± 0.7	80 ± 0.05

Table 1: Geometric distribution of branches of interest

.

"

L202 Is the different growth kinetics and other parameters you analyse (lightly vs heavily loaded branches) related to the height of the branch in the crown? Or their age? This might give new perspectives to the paper going more into biological implications.

The reviewer is right. Our model could be very useful in order to study the relationship between the biological parameters of the branches and their mechanical constrains. This is one of the exiting prospects of this work. Actually, we did few preliminary tests. For example, we tried to enlighten the relationship between external parameters and the growth kinetic of branches. See the results in the figure below that depicts the variation of ν_M, λ_M vs geometrical parameters L, r, and the insertion angle θ.

For *Pinus*, no particular correlation has been found. In the birch tree, some particular pattern distribution has been found: the range of variability of growth kinetic seems to increase, then decreases after reaching a peak (as the length and radius of branches increase).

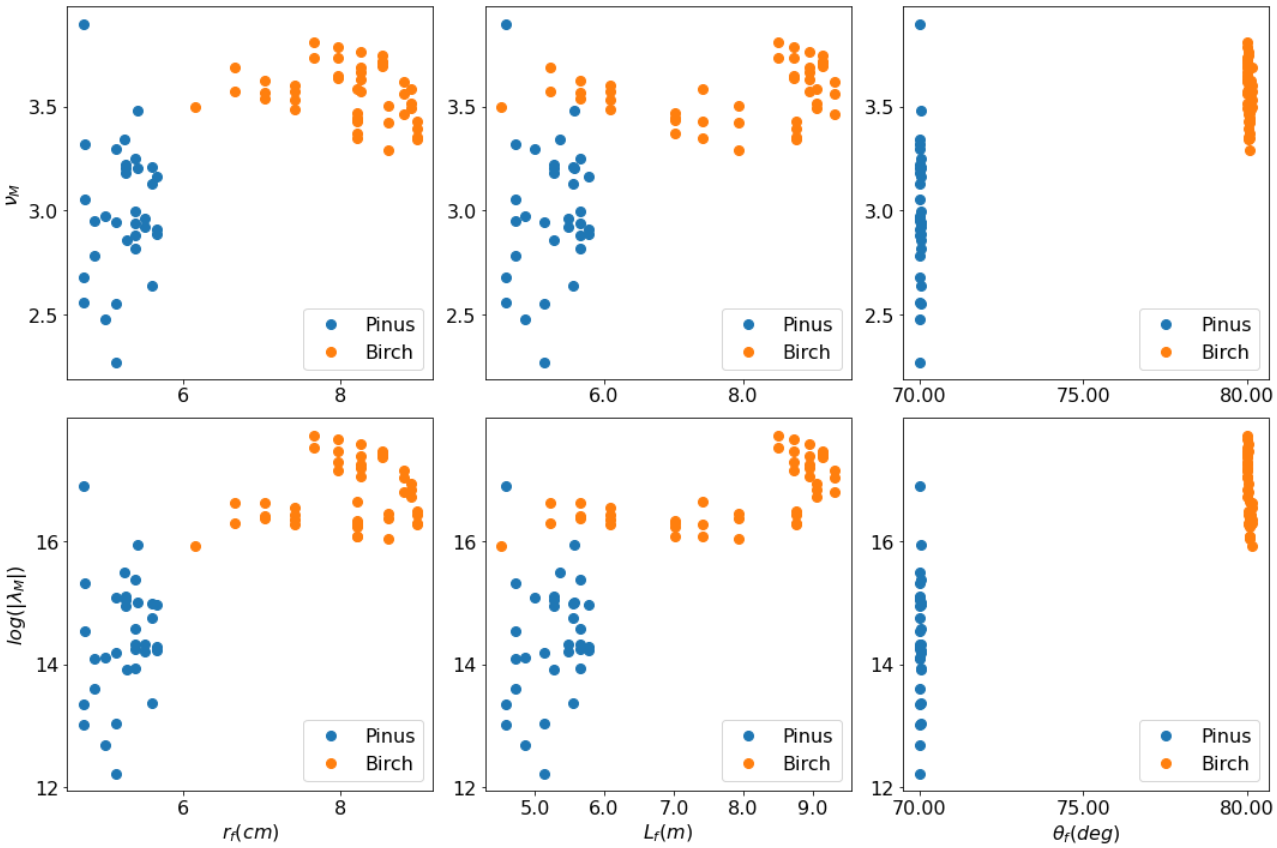

Also, following the reviewer's suggestion, we looked at the variations of ν_M, λ_M with age and branch position in the crown. The results are presented in the figure below. Again, for *Pinus*, no particular correlation was found, either for the age of for the insertion height. For *Prunus,* the growth kinetics seem to decrease with the age, while the range of variability of the branch weight (λ_M is linked to the weight) decreases. This means that the old branches tend to the same bending moment, with the same length to radius ratio. An interesting graph is given below. It shows the dependency on the insertion height. The branches in the middle of the crown are the heaviest ones (even if 14m seems to be the highest insertion height, it is just for branches older than 20 years; the crown goes up until 18m).

Again, we totally agree that we could play with the model in order to study many biological hypotheses and their consequences. However, this paper is a first step that depicts the model. We just used few examples in order to illustrate the power of such modelling approach. Moreover, we think it would be more relevant to use real experimental data for the description of branches than simulations that are always questionable. This open exiting prospect for further collaborations between biomechanicians and biologists.

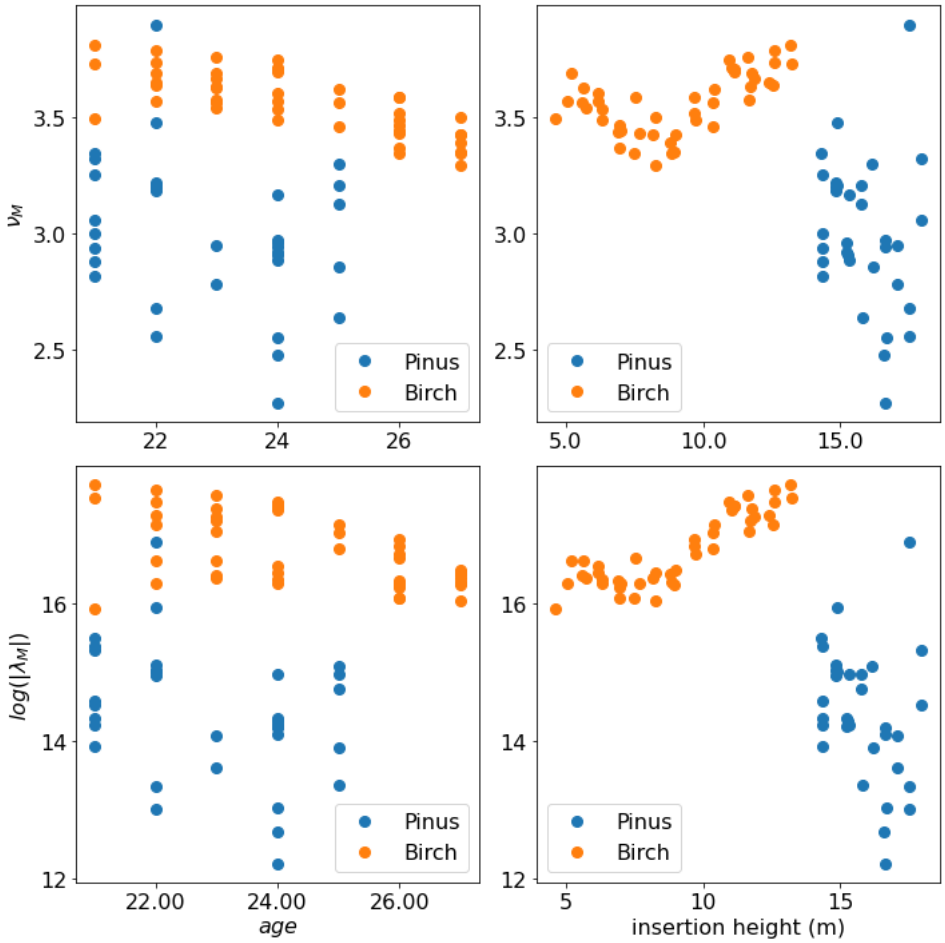

L205 How do you interpret this variability in the loading history? How the change in branch angle is handled in the model if it is handled?

The comment is relevant: the variability could be linked to the branching of branches, which may be related to the position of the branches in the crown. Here, the branches angle is generated by the AMAP-sim simulator and is based on huge dataset measured by botanists. Please look at answer of L222 for more information.

L206 It would be better to presents both variations in relative or absolute values, not a mix.
The reviewer is right and in the new version, we have reworded this part in this way (L212-221).
L212:
"For the selected branch groups, the distribution of all allometric coefficients are presented in Fig 4. In Pinus, there was a large variation in $\nu-$coefficient, with ν_M varying by almost a factor 2 in the studied sample; indicating very variable secondary growth kinetics. In Prunus, the range of variation of the allometric power coefficients was smaller, which depicted a higher homogeneity of secondary growth kinetics. For both species, a great diversity in $\lambda-$coefficients was observed; which depicted a significant variability in the loading history. This is particularly interesting as the branches showed geometric determinants that did not vary over large ranges (Table 1). Also, these coefficients do not appear to vary as a function of geometric parameters. This reflects the complexity of predicting the loading of a branch from the determinants of the main axis, and shows the importance of branching. In both cases, these variations in the $\lambda-$coefficients result in a factor of 4 in the bending load between the lightly loaded and the heavily loaded branches."

L213 Stem orientation?
It was a mistake (probably a wrong copy). This was removed.

L222 It might be interesting to have an idea about the branch angle at insertion; can you extract them from the model of loading and look at its variability?

On the followed figure, we plotted the final insertion angle for all branches which are inserted directly to the trunk (whatever their age). As you can see, after the first stage of growth (> 10 years) this insertion angle became uniform. Following our discussions with the botanists of the AMAP team, this plateau is close from the distribution in real trees.

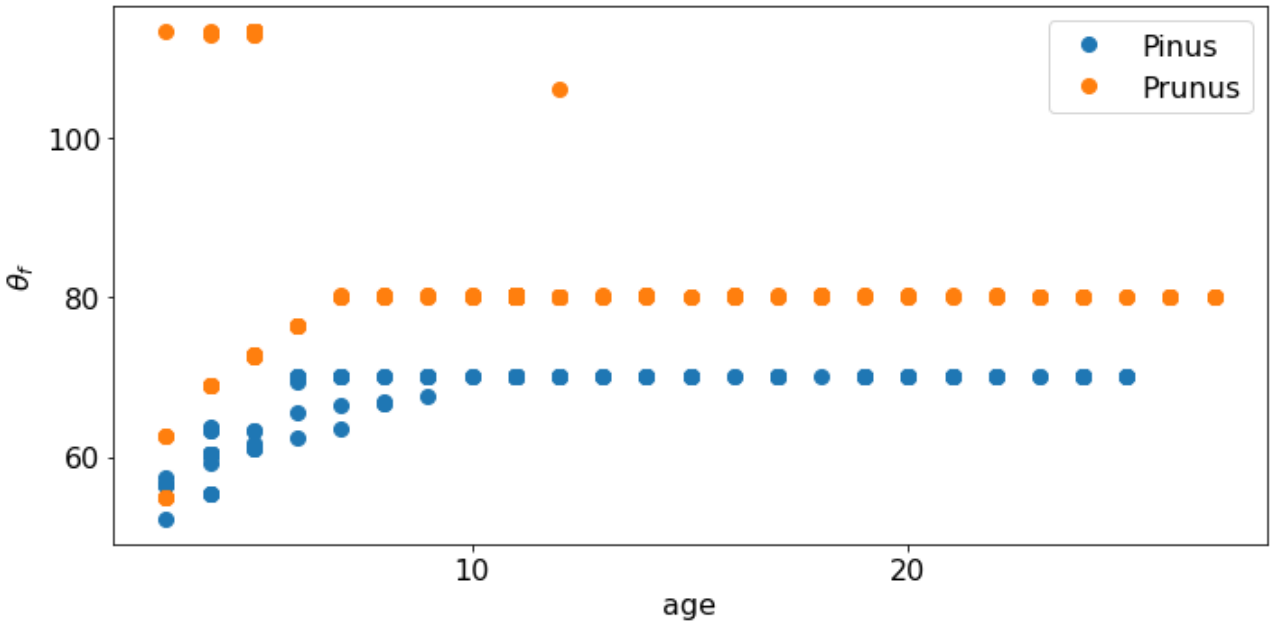

L231 both strategies alone – reword
Done: we changed (see L288): "using either eccentric growth or RW led to ..."

L235 Eccentricity of 0.6 is already very high
Indeed, we have changed all the discussion about this point, including comparison with personal data and literature. Eccentricity must be analysed taking into account an offset: see L288-302 for more information.

L239 The more space eccentricity leaves to TW – please reword, it is not very clear
change modified: for example:

- in L250: "The more hypotrophic the eccentricity, the higher the tension stress at periphery."
- in L313: "a higher maturation stress led to a larger eccentricity"

L247 Please introduce results you are describing. Less intense TW reword lower ☒ TW
According to the suggestions of the reviewers and editor, we modified the structure of the paper and we split the "result and discussion" section into 2 separate parts.

L245 Which trade-off is on your mind?

This may be construction costs (biomass costs) or hydraulic constraints.

L315-320: "However, experimental observation showed that this is not the usual configuration for branches. It raises interesting question on the main mechanical driver of branch construction. From a biological point a view, it could be more "costless" to produce TW than eccentricity, but this

hypothesis was not yet investigated. Also, more work is needed to understand how TW and eccentricity are linked in angiosperm trees: since they may have some uncoordinated action, we can wonder if they have common triggered factors."

L255 ability -> capacity
Corrected
L263 inclination reword microfibril angle
Corrected

L269 eccentricity of 0.8 is very high, you previously mentioned that posture control drivers are less triggered but eccentricity modelled here is higher in softwood than in hardwood

This part was a bit ambiguous. By 'less triggered', we meant that the softwood branches were lighter than the hardwood ones. But even if the loading is lower, the eccentricity needed to counteract this loading is higher. We hope that the formulation is clearer in the new version (L322):

"First of all, the values of the stress distribution were much lower than for Prunus avium. This was explained by the size of the modelled branches: the average bending moment is much higher for birch tree than for pine, by a factor roughly 10. The effect of each factor alone (Fig 7) suggested that maturation is a much more efficient option than eccentricity. To ensure the same growth scenario, the eccentricity alone rose to about 0.8, which is close to a theoretical limit, whereas maturation alone led to low maturation strains in CW (<500 mu strain, corresponding to 4 MPa)."

L267 I am wondering why do you let your model go for epitrophic eccentricity in conifer branches as this is not observed in nature. We do not need a complicated model to understand that allocation of the biomass to the lower side of the branch is not efficient mechanically.

Actually, one of the limits of the model is the homogeneous stiffness. If we wanted to be more realistic, we have to compensate this hypothesis by considering a 'compensating eccentricity' (we can see this as an initial eccentricity, like an offset). Therefore, our epitrophic eccentricity could be offset and become hypotrophic. We added a paragraph (L371-388) and a figure (Fig 11) to give more details on this point.

L274 What do you mean by coordination problem?

In the new version, we changes the whole part of the analyse that refered to this point and this expression is not available anymore. However, by "coordination problem", we meant that during the first stage of development, when CW is not yet differentiated, the eccentricity should be epitrophic, and then hypotrophic (as soon as the absolute value of CW is greater than NW). This small delay and theoretical change in the sign of eccentric growth could be a coordination problem. But we removed this part from the new discussion. More experimental work would be needed to investigate the role of these two parameters at the beginning of the growth.

L277 In case of combined effects – specify the scenario, same for L286, by the way you start to discuss Fig. 8b before Fig. 8a
Corrected

L278 I can not see any red dotted line in Fig. 8b
We changed the whole figure (see answer to the first reviewer)

L284 It is a bit surprising conclusion because in general in temperate softwood branches exhibit more eccentric growth compared to temperate hardwood species.
See the new formulation. We think that eccentric growth does not play a crucial role in the control of the orientation. It is probably triggered by other factors. Also, from what we observed in experimental data recorded in our lab (not published yet), temperate softwood branches do not exhibit more eccentric growth than temperate hardwood species.

L295 This section is not very clear to me: Generating some tension at the pith allows the branch to create more CW...you mean that softwood branch could produce tension wood at the beginning of its growth under assumption of epitrophic growth? This seems to me rather unrealistic scenario for a softwood branch, I am not sure we should go for a deeper analysis you suggest for that but maybe I misunderstood?
Indeed, softwoods do not produce tension wood, but any stress can be produced in the already formed wood as a result of the formation of the later layers. Usually in the pith compression stress is produced, which makes the situation of produced tension in the pith quite unusual, but it was an outcome of the simulation

Fig. 9 – I do not think this figure gives additional information compared to Fig. 8
The comment was relevant. We remove the figure.

L307 Replace straightening by uprighting here
Corrected

L313 Expression building of branches should be revised
In the whole document, we changed “building” by “construction”.

L314 Ok for bending due to self-weight however any little wind sway will change everything.
Of course wind change everything and this could obviously be a perspective of the work. We actually have coupled our model with some horizontal bending momentum, and included a horizontal eccentricity too. But it is another (part of the) story!

L323 I am wondering if the shape change could not be an issue as well for perspectives, to test behaviour of ovalized cross-section of branches for example.
Indeed that would be an interesting perspective. The cross-section provided by the Amap simulator were circular.This was not possible to consider oval sections in this work. Since only the vertical bending was considered, ovalized cross-section do not make much difference, except in terms of weight: vertical ovalization would be beneficial for the bending rigidity to weight ratio, while horizontal ovalization (sometime observed in plagiotropic branches) should improve the lateral resistance to wind.

Modelling the growth stress in tree branches: eccentric growth *vs.* reaction wood ~~impact of different growth strategies~~

A. Van Rooij[1,2], E. Badel[2], J.F. Barczi[3], Y. Caraglio[3], T. Alméras[4] and J. Gril[1,2]

1. Université Clermont-Auvergne, CNRS, Institut Pascal, F-63000, Clermont-Ferrand, France
2. Université Clermont-Auvergne, INRAE, PIAF, F-63000, Clermont-Ferrand, France
3. CIRAD, UMR AMAP, F-34398 Montpellier, France.
AMAP, Univ Montpellier, CIRAD, CNRS, INRAE, IRD, Montpellier, France.~~CIRAD, Unité Mixte de Recherche (UMR) Cirad-Cnrs-Inrae-Ird-Université Montpellier 2, 'botAnique et bioinforMatique de l'Architecture des Plantes' (AMAP), A-51/PS2, Boulevard de la Lironde, 34398 Montpellier cedex 5, France~~
4. LMGC, CNRS, Université of Montpellier, Montpellier, France

Abstract

This work aims to model the mechanical processes ~~the mechanical consequences of different strategies~~ used by tree branches to control ~~ensure~~ their posture despite their increasing weight loading ~~the increasing loading due to gravity.~~. The two known options ~~strategies~~ for a branch to maintain its orientation ~~straighten itself~~ are the asymmetry of maturation stress, including reaction wood formation, and eccentric radial growth. Both options ~~strategies~~ can be observed in nature and influence the stress distribution developed in the branch each year. This so-called "growth stress" reflects the mechanical state of the branch. In this work, a growth stress model was developed at the cross-section level in order to quantify and study the bio-mechanical impact of each process ~~strategy~~. For illustration, this model was applied to ~~the~~ branches of two 50-year-old trees, one softwood *Pinus pinaster* and one hardwood *Prunus avium*, both simulated with the AMAPSim finite element software. The computed outputs enlightened that, for both *Prunus avium* and *Pinus pinaster*, eccentric radial growth is less efficient than the formation of reaction wood to counter increasing gravity stress applied to the branch. For the pine, although eccentric growth does not necessarily act as a relevant lever for postural control, it greatly modifies the profile pattern of mechanical stress and could provide mechanical safety of the branch. This work opens experimental perspectives to understand the biomechanical processes involved in the formation of branches and their mechanical safety. ~~The model show that in hardwoods, both strategies are efficient and that the combination of the two is optimal. In softwoods, the model shows that eccentricity process is less efficient. Moreover, eccentricity process does not necessarily act as a relevant lever for postural control. However eccentricity process greatly modify the profile pattern of mechanic stress. This work opens exciting experimental perspectives in order to understand the biomechanical process involved in the building of branches.~~

Abbreviations and notations (in order of occurrence)

NW,TW,CW	Normal Wood, Tension Wood, Compression Wood
(x, y, z)	Local reference coordinates ~~system~~ associated with the section
O	Centre of the section
r, R	Radial polar coordinate and Radii of the cross section (m)
$e(R), \overline{e(R)}$	Eccentricity at the stem radius R, integrated eccentricity up to r = R
(x', y', z')	Local reference coordinates associated with the section, centred on the pith
σ	Stress (MPa)
σ_0	Induced maturation stress (Mpa)
S	Cross section area (m^2)
N, M	Loads (N): normal force parallel to z' and bending moment around y'
E	Module of elasticity in L direction (GPa): MOE
μ	Induced maturation strain
ϵ, a, b	Strain,~~Deformations:~~ at the center, ~~changes in~~ local curvature ~~around x,y~~
K_i	Structural stiffness of the cross-section
F_i	External coefficients (maturation and load)
θ	Circumferential position in section (rad)
$\sigma_0(\theta)$	Maturation strain in the new ring at circumferential position θ
α	Mean maturation stress in the new ring
β	Differential stress in the new ring
$R_{x'y'}$	Radius of the cross section at the instant of appearance of the point (x', y')
$\lambda_N, \lambda_M, \nu_M, \nu_N$	Load power law: allometric coefficient
λ_b, ν_b	Change of curvature power law: allometric coefficient
$\sigma_{NW}, \sigma_{TW}, \sigma_{CW}$	Maturation stress in the normal wood, tension wood and compression wood
$\mu_{NW}, \mu_{TW}, \mu_{CW}$	Maturation strain in the normal wood, tension wood and compression wood
$\overrightarrow{N_n}, \overrightarrow{M_n}$	Loads of growth unit n: normal force and bending moment around y
N_z, M_x, M_y, M_z	Loads of growth unit n: projection of $\overrightarrow{N_n}$ on $\vec{z}$ and bending moment $\overrightarrow{M_n}$ around $\vec{x}, \vec{y}, \vec{z}$
m_n	Mass of the growth unit n (kg)
g	Gravity constant: $g = 9.8$ m.s^{-2}
G_n	Centre of gravity of the growth unit n
E_d, E_g	Air-dry, green MOE
ρ	Density
μstrain	$1/10^6$
D_n, D_{n+1}	First and second diameter the growth unit n
D_f	Deflection of a growth unit
L_n	Length of the growth unit n

Introduction

From a mechanical point of view, wood in tree fulfils three major functions: construction of the tree architecture, postural control of trunk and branches and breaking resistance to external stimuli ~~construction of the architecture, postural maintenance and resistance to external elements~~ [Thibaut (2019)]. These three functions are provided by the way wood cells differentiate and accumulate during wood formation process. Each axis of a tree can be considered as an inclined beam, consisting of a succession of conical growth units [Barthélémy and Caraglio (2007)]. It is built in two steps: first, primary growth resulting in new growth units that increase the length of the initial axis; and secondary growth resulting

in thickening of already existing units by addition of annual rings. These two interactive and additional processes lead to a specific pattern of mechanical stress, called 'growth stress', which can be analysed as the superposition of support stress and maturation stress [Archer (1976); Fournier et al. (1991a)]. The support stress results from the continuous increase of the weight supported by the axis over the years. It reaches maximal levels in the core of the stem and vanishes near stem periphery, where the recently formed wood contributes to the support of recently produced biomass only. Maturation stress is set up at the end of the cell-wall maturation process, when molecular components such as lignin polymerise, generating growth forces by small dilatation or contraction restrained by the rigidity of the previously formed wood cells [Alméras and Clair (2016)]. An evaluation of the maturation stress can be obtained by measuring the strain associated to stress release at stem periphery, where no support stress is present [Nicholson (1971); Yoshida and Okuyama: (2002); Yang et al. (2005)]. The circumferential heterogeneity of this peripheral stress is needed to regulate stem curvature. In most cases, a tensile maturation stress is produced in the newly formed 'normal wood' (NW). But observations on inclined trunks [Alméras et al. (2005); Coutand et al. (2007); Thibaut and Gril (2021)], seedlings [Hung et al. (2016)] and branches [Fisher and Stevenson (1981); Huang et al. (2010); Tsai et al. (2012); Hung et al. (2017)] have evidenced a clear difference between hardwoods and softwoods behaviour~~trees~~. Hardwoods are able to produce 'tension wood' (TW) inducing a much higher tensile stress on one side, while for softwoods a compressive stress is induced in 'compression wood' (CW). The first pulls, the second pushes. In the most usual cases of inclined stems restoring their vertical orientation, TW is formed on the upper side while~~and~~ CW is formed on the lower side of the trunk. But other situations can be encountered depending on the biomechanical requirements of the tree [Wang et al. (2009b)]. In addition to their participation in the postural control of tree stems, these two types of so-called 'reaction wood' (RW) are characterised by specific~~a different~~ anatomical pattern (not discussed here) and specific physical and mechanical properties.

As an alternative to complex experimental approaches, growth stress modelling plays an important role in the understanding of the phenomena involved in the orientation process of a stem. The history of biomechanical models began ~~begins~~ with Kübler (1959) who proposed an analytical formulation of growth stress for a perfect cylinder made of a homogeneous and transversally isotropic wood.

Later, Archer and Byrnes (1974) took into account an asymmetry of the maturation stress, and Fournier et al. (1991a,b) proposed a semi-incremental version of these models, allowing to take into account a potential gradient of mechanical parameters (stiffness, maturation). By associating their previous model to the loading induced by the tree weight, Fournier et al. (1994) made the connection between growth stress and stem orientation. ~~To understand the parameters involved in orientation of the stems,~~ This model has been adopted and developed by several authors in order to study the orientation process of stems. Yamamoto et al. (2002) added a primary shoot and returned to curvature calculations. Alméras and Fournier (2009) introduced the notion of gravitropic performance (capacity of the tree to correct the bending moment induced by its weight) and proposed criteria of long-term stability. Huang et al. (2005) and Alméras et al. (2005) impoved~~made~~ the model by introducing a secondary growth asymmetry and its resulting pith eccentricity, as well as stiffness heterogeneity, allowing to ~~them~~ quantify the effectiveness of eccentricity, maturation, stiffness gradient and initial radius in the curvature regulation process. They ~~both~~ enlightened~~showed~~ that the main factor in the gravitropic ~~correction~~ process is the spatial distribution of the maturation stress. Still in line with Fournier's 1994 model, Alméras et al. (2018) recently developed analytical models of longitudinal growth stress, taking into account different configurations, like eccentricity or maturation gradient, and evolution laws, like evolution of stiffness per additional layer. Finally, based on the same philosophy as ~~that~~ established by Kübler, tree-scale and finite-element models have emerged [Fourcaud et al. (2003); Ancelin et al. (2004)].

Huang et al. (2010)'s model has been used to understand how eccentric growth and reaction wood are involved in branch orientation [Huang et al. (2010); Huang et al. (2009a); Huang et al. (2012); Huang et al. (2017)],

but all theses studies were based on the current state of the branch, without consideration of the previous history: although some of them quantified the roles of maturation and eccentricity in the regulation of curvature, none did evaluate their capacity to ensure a given growth scenario.~~Most of these models have been applied to trunks. Some theoretical work have been done for on inclined trunks [Alméras and Fournier (2009)]; and only one analytical work has been done so far on branches [Huang et al. (2010)]. Branches are particular axes subject to large inclinations, and some assumptions such as uniformity of eccentricity find their limits.The only model including an integration of the stress on the whole section, was proposed by Fourcaud et al. (2003),but did not take into account the eccentricity.Huang et al. (2~~ ~~and Alméras et al. (2005) have quantified the roles of maturation and eccentricity in the recovery process, but did not evaluate their capacity to ensure a given growth scenario.~~.

Unlike trunks, which usually seek verticality, after the first stages of growth, branches tend to grow in a stationary way at a fixed angle to the vertical. Therefore, in this framework,~~In this framework,~~ we are interested in understanding how branches can control their orientation, through the study of growth parameters: eccentric growth and reaction wood. The aim is to check by calculation what option is mechanically possible and safe for the branch. For this purpose, we developed a semi-incremental biomechanical model of growth stress at the cross section level that takes into account the eccentricity and maturation gradients during the building of branches. Using the digital models of one softwood *Pinus pinaster* and one hardwood *Prunus avium* ~~a hardwood and a softwood~~, the impact of each of these two growth parameters ~~straightening strategies~~ on the stress state were evaluated.

Material and methods

Numerical model

General hypotheses

The problem ~~will~~ was set in the framework of the beam theory. From a geometrical point of view, branches generally show profiles that ~~are well~~ suit to this type of analytical framework: a slender shape and no important diameter variations. The shape effects due to twigs and other local biological phenomena (cavity, nodes, etc.) were neglected. The same set of hypotheses as in Alméras et al. (2018) was adopted. In this study, we focused on the behaviour in the longitudinal direction (parallel to the main axis). Horizontal bending and torsion loads were not considered. Only the vertical bending moment (~~that~~ caused by the weight) was considered; these ~~initial~~ hypotheses on the loading modes are discussed later.

Geometrical settings

The object of study was the cross-section of a branch, placed within a plane locally orthogonal to the pith. The local reference frame of the section is $(\vec{x}, \vec{y}, \vec{z})$, with $\vec{z}$ the longitudinal direction of the axis, and $\vec{x}$ placed in a vertical plane and facing upwards (Figure 1). The shape of the cross-section was assumed to be circular at any stage of development, described by the successive depositions of wood rings. The term of 'ring' refers here to the volume occupied by wood cells produced by the cambium during a certain duration of time, not necessarily annual: it must be taken in a numerical meaning~~sense~~. These rings possibly could present an eccentricity resulting from asymmetry of secondary growth. Since the model only takes into account vertical bending, the eccentricity was set along the x axis, as expressed by the following equation:

$$O(t) = \int_0^{R(t)} e(r)dr = \overline{e}R(t) \tag{1}$$

with $O(t)$ the position of the geometrical centre and $R(t)$ the radius of the section at time t, e(r) the eccentricity when the stem radius was r and $\overline{e}$ the integrated eccentricity up to $r = R$. The eccentricity can vary in the interval $[-1, 1]$. A zero eccentricity corresponds to a centred section, while -1 or 1 corresponds

to maximum eccentricity resulting from secondary growth only on the lower or the upper side of the section, respectively. In the following, the position x' in the pith reference frame is~~will be~~ needed. By calling x the vertical position in the geometrical reference frame, we deduce from equation 1:

$$x = x' - \bar{e}R \tag{2}$$

Computation of the mechanical behaviour

We ~~will~~ developed a radial incremental method. For each radial increment, the longitudinal stress was computed in order~~so as~~ to satisfy the static equilibrium of the cross section:

$$\begin{cases} \int_S \delta\sigma dS + \int_{\delta S} \sigma_0 dS = \delta N & \text{(3a)} \\ \int_S \delta\sigma x dS + \int_{\delta S} \sigma_0 x dS = -\delta M & \text{(3b)} \end{cases}$$

where S is the cross-section area, δS is its increment, $\delta\sigma$ is the increment of stress σ in the already formed wood, in response to the maturation stress σ_0 generated in the new wood layer. δN and δM are respectively the increment of external force N and bending moment M, that are applied on the cross-section. For illustration, the geometric situation for K rings and an increment of stem radius δR is proposed in Figure 1.

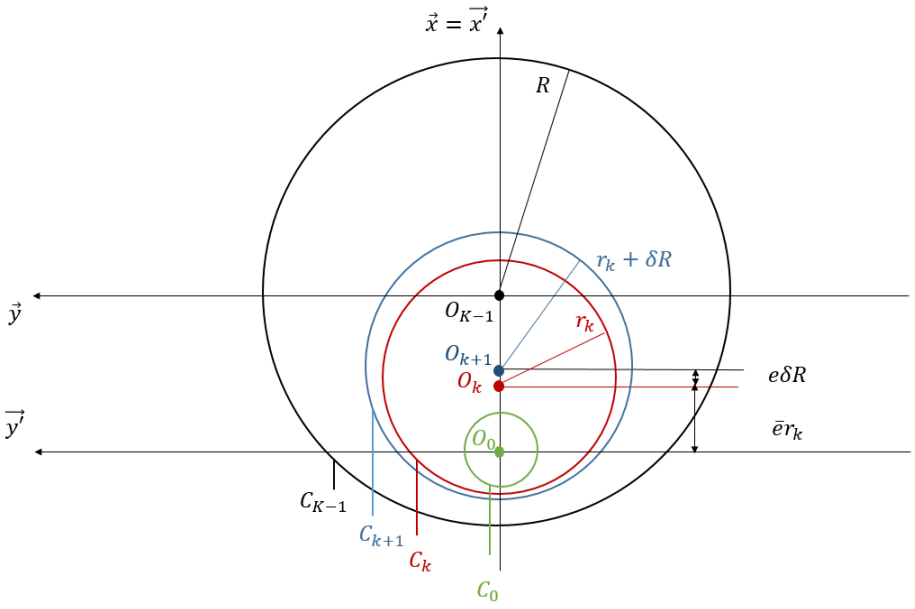

Figure 1: Geometrical representation of a section with K numerical rings and a radial increment δR between rings $(k-1)$ and k.

The stress σ is linked to the strain ϵ by a classical pre-stressed Hooke law:

$$\sigma = E\left(\epsilon - \mu\right) = E\epsilon + \sigma_0 \tag{4}$$

where E is the longitudinal Young's modulus, μ is the maturation strain and σ_0 is the maturation stress. In the context of the beam theory, the planar sections remain planar ~~sections~~ (Euler-Bernouilli assumption). The strain field is then described by the deformation a at the centre of the pith and the curvature b relative to the y-axis as follows:

$$\delta\epsilon = \delta a + x\delta b \tag{5}$$

where $\delta\epsilon$, δa, δb are the increments of ϵ, a, b, respectively. The stress increment $\delta\sigma$, in the already formed wood, where no maturation occurs anymore, can then be deduced:

$$\delta\sigma = E\delta\epsilon = E(\delta a + x\delta b) \tag{6}$$

From these considerations, the system (3) becomes (details of the calculation are given in Appendix A):

$$\begin{cases} K_0\delta a + K_1\delta b = \delta F_0 & \text{(7a)} \\ K_1\delta a + K_2\delta b = \delta F_1 & \text{(7b)} \end{cases}$$

with

$$K_0 = E\pi R^2, \quad K_1 = E\pi\overline{e}R^3, \quad K_2 = E\pi R^4\left(\overline{e}^2 + \frac{1}{4}\right) \tag{8}$$

$$\delta F_0 = -\int_{\delta S}\sigma_0 dS + \delta N, \quad \delta F_1 = -\int_{\delta S}\sigma_0 x dS - \delta M$$

The calculation of the coefficients δF_0 and δF_1 depends on the formulation of the maturation stress. The maturation stress was assumed to vary circumferentially as follows:

$$\sigma_0(\theta) = \alpha + \beta\cos\theta \tag{9}$$

where the mean stress α and differential stress β were defined differently in softwood and hardwood species:

$$\begin{cases} \text{Hardwood: } \alpha = \dfrac{\sigma_{TW} + \sigma_{NW}}{2}; \beta = \dfrac{\sigma_{TW} - \sigma_{NW}}{2} & \text{(10a)} \\ \text{Softwood: } \alpha = \dfrac{\sigma_{CW} + \sigma_{NW}}{2}; \beta = \dfrac{\sigma_{NW} - \sigma_{CW}}{2} & \text{(10b)} \end{cases}$$

where σ_{TW} (resp. σ_{CW}) is the maturation stress in the tension wood (resp. compression wood), and σ_{NW} is the stress in the opposite wood (normal wood). One gets :

$$\begin{cases} \delta F_0 = -\pi R\left(2\alpha + e\beta\right)\delta R + \delta N & \text{(11a)} \\ \delta F_1 = -\pi R^2\left(3\alpha e + e^2\beta + \beta\right)\delta R - \delta M & \text{(11b)} \end{cases}$$

From equations (8), (11a) and (11b), the components of the system (7) are known. By inversion, $\delta\alpha$ and δb can be obtained according to the following equations (see details in Appendix B):

$$\begin{cases} \delta a = \dfrac{4}{ER}\left[\left(3e\overline{e} - 2e^2 - \dfrac{1}{2}\right)\alpha + \left(\overline{e}e^2 - e\overline{e}^2 + \overline{e} - \dfrac{e}{4}\right)\beta\right]\delta R + \dfrac{4}{E\pi R^3}\left[\overline{e}\delta M + \left(\overline{e}^2 + \dfrac{1}{4}\right)R\delta N\right] & \text{(12a)} \\ \delta b = \dfrac{-4}{ER^2}\left[\left(3e - 2\overline{e}\right)\alpha + \left(e^2 - e\overline{e} + 1\right)\beta)\right]\delta R - \dfrac{4}{E\pi R^4}\left(\delta M + \overline{e}R\delta N\right) & \text{(12b)} \end{cases}$$

Once δa and δb are known, the stress increment $\delta\sigma$ at any position given by (x', y') can be obtained from equation(6). The stress distribution at this position can be obtained as the sum of the initial maturation stress and all the stress increments undergone by the material point since its creation.

$$\sigma(x', y', R) = \sigma_0(x', y') + \sum_{k=k_{x'y'}}^{K}\delta\sigma_k \tag{13}$$

where $\delta R_k = r_k - r_{k-1}$ for a succession of ring radii $0 < r_0 < ... < r_k < ... < r_K = R$, $\delta\sigma_k$ is the corresponding increment, and $k_{x'y'}$ designates the ring containing the point.

Analytical formulations

Using equations (12b) and dividing by dR, we get the following equations when dR tends to zero~~When each incremental term in expression (12b) is divided by dR and dR tends to zero, the ratio tends to the derivative against R, leading to~~ :

$$\begin{cases} \dfrac{\mathrm{d}a}{\mathrm{d}R} = \dfrac{4}{ER}\left[\left(3e\overline{e} - 2e^2 - \dfrac{1}{2}\right)\alpha + \left(\overline{e}e^2 - e\overline{e}^2 + \overline{e} - \dfrac{e}{4}\right)\beta + \dfrac{1}{\pi R^2}\left(\overline{e}\dfrac{\mathrm{d}M}{\mathrm{d}R} + \left(\overline{e}^2 + \dfrac{1}{4}\right)R\dfrac{\mathrm{d}N}{\mathrm{d}R}\right)\right] & (14a) \\ \dfrac{\mathrm{d}b}{\mathrm{d}R} = \dfrac{-4}{ER^2}\left[\left(3e - 2\overline{e}\right)\alpha + \left(e^2 - e\overline{e} + 1\right)\beta + \dfrac{1}{\pi R^2}\left(\dfrac{\mathrm{d}M}{\mathrm{d}R} + \overline{e}R\dfrac{\mathrm{d}N}{\mathrm{d}R}\right)\right] & (14b) \end{cases}$$

Using equation (13) and dividing by δR, we obtain the following spatial derivative equation $\partial\sigma/\partial R$: ~~If the division by δR is applied to the stress σ, a function of the stem radius R and the position x', the partial derivative $\partial\sigma/\partial R$ is obtained, so that equation (13) becomes:~~

$$\sigma(x', y', R) = \sigma_0(x', y') + \int_{R_{x'y'}}^{R} \frac{\partial\sigma}{\partial R}(x', R')dR' \quad (15)$$

where~~by calling~~ $R_{x'y'}$ is the radius of the section at the instant of appearance of the point with coordinates (x', y').

On the other hend, the expressions of axial force $N(R)$ and bending moment $M(R)$ are required~~needed~~ to compute the evolution of the stress distribution in the cross section. For this purpose, we assumed that both~~they~~ vary as a power function of the radius of the branch. This resulted in the following allometric laws:

$$\begin{cases} N = \lambda_N R^{\nu_N} & (16a) \\ M = \lambda_M R^{\nu_M} & (16b) \end{cases}$$

with $\lambda_{N,M}$ and $\nu_{N,M}$ are allometric coefficients. The $\lambda-$coefficients are directly proportional to the weight of the branch part supported by the cross section (the branch itself and the other axes of higher orders). The $\nu-$coefficients express the kinetics of the secondary growth: a small ν refers to an early secondary growth while a higher one refers to a later diameter increase.

The calculation of σ requires also the knowledge of the temporal variation of thecurvature b. In order to simplify the analyses, we mainly studied stationary cases~~most of the cases, e we will assume~~ i.e. we assumed that the branch maintains its orientation and remains straight. This assumption results in $\dfrac{\mathrm{d}b}{\mathrm{d}R} = 0$. ~~and the fact that~~ Physiologically, this equation expresses that the branch always compensates ~~balances~~ its weight increment at eachevery deposition step of a new wood layeraddition. However, we can consider two cases for which the branch does not build up in a stationary way: i) the passive bending (under its own weight) case, and ii) the up-righting case (i.e. the action of maturation is stronger than the additional weight). In both cases, the resulting change in curvature has been modelled~~calculated~~ by Alméras and Fournier (2009) and Alméras et al. (2018). It can then be written as follows:

$$\begin{cases} \text{Up-righting:} & \dfrac{\mathrm{d}b}{\mathrm{d}R} = -4\dfrac{\beta}{ER^2} & (17a) \\ \text{Passive bending:} & \dfrac{\mathrm{d}b}{\mathrm{d}R} = 4\dfrac{\lambda_M\nu_M}{E\pi}R^{\nu_M - 5} & (17b) \end{cases}$$

For the next computations~~calculation~~, we used the following~~will then take a~~ general law:

$$\frac{\mathrm{d}b}{\mathrm{d}R} = \lambda_b R^{\nu_b} \quad (18)$$

Combining (14),(15),(16) and (18), the total stress can then be computed as:

$$\sigma^i(x',y',R) = \sigma_0^i(x',y') + S_1 \ln\left(\frac{R}{R_{x'y'}}\right) + \frac{S_2}{S_3}\left(R^{S_2} - R_{x'y'}^{S_2}\right) + \frac{S_4}{S_5}\left(R^{S_5} - R_{x'y'}^{S_5}\right) + \frac{S_6}{S_7}\left(R^{S_7} - R_{x'y'}^{S_7}\right) x' \quad (19)$$

where $S_1 = 4\left[\left(3e\overline{e} - 2e^2 - \frac{1}{2}\right)\alpha + \left(\overline{e}e^2 - e\overline{e}^2 + \overline{e} - \frac{e}{4}\right)\beta\right]$ is driven by the maturation process, $S_2 = \frac{\lambda_N \nu_N}{\pi}\left(\overline{e}^2 + \frac{1}{4}\right)$, $S_3 = \nu_N - 2$, $S_4 = \frac{4}{\pi}\lambda_M \nu_M \overline{e}$ and $S_5 = \nu_M - 3$ by branch loading (geometric evolution of the branch), $S_6 = E\lambda_b$ and $S_7 = \nu_b + 1$ by the orientation of the branch.
For each radius r, the remaining unknowns are the mean stress α, the differential stress β and the eccentricity e. Equation (14b) can be rewritten as:

$$(3e - 2\overline{e})\,\alpha + \left(e^2 - e\overline{e} + 1\right)\beta = \frac{-1}{\pi r^2}\left(\frac{dM}{dR} + \overline{e}R\frac{dN}{dR}\right) - E\frac{R^2}{4}\frac{db}{dR} \quad (20)$$

Thus by fixing two parameters, the third is directly determined. The maturation parameters α and β are determined by the maturation stress σ_{NW} in normal wood and σ_{TW} or σ_{CW} in reaction wood according to equation (10). ~~these parameters will be managed~~.
We considered~~will consider~~ two possible configurations for the simulations in next section:

1. First, we applyed a constant eccentricity (so that $\overline{e} = e$) and we fixed the stress level in the normal wood. In that case, the maturation stress of the reaction wood was given by equations (10):

$$\begin{cases} \sigma_{TW} = \dfrac{-2}{\pi R^2(1+e)}\left(\dfrac{dM}{dR} + er\dfrac{dN}{dR}\right) + \sigma_{NW}\left(\dfrac{1-e}{1+e}\right) + \lambda_b\left(\dfrac{ER^2}{2(1+e)}\right)R^{\nu_b} & (21a) \\ \sigma_{CW} = \dfrac{2}{\pi R^2(1-e)}\left(\dfrac{dM}{dR} + eR\dfrac{dN}{dR}\right) + \sigma_{NW}\left(\dfrac{1+e}{1-e}\right) - \lambda_b\left(\dfrac{ER^2}{2(1-e)}\right)R^{\nu_b} & (21b) \end{cases}$$

2. Second, we fixed the maturation parameters and we observed how the eccentric growth could, or not, maintain the orientation of the branch. ~~we observe how the branch straighten, or not, just by varying the eccentricity of the secondary growth.~~ In this configuration, equation 20 becamebecomes a two degrees equation in e that could be solved numerically.

In these two configurations, using data on the support allometries $\lambda_N, \lambda_M, \nu_M, \nu_N$, we can calculate the stress in the reaction wood and/or the eccentricity with different (λ_b, ν_b), then deduce the growth stress profile in the section (eq. 19). In the next part, we see how the allometric coefficients can be obtained from data generated by growth model~~realistic growth data~~.

Realistic growth data

Tree architecture modelling~~Tree material~~

Numerical experiments were carried out using two reference models: one softwood *Pinus Pinaster* (pine) and one hardwood *Prunus avium* (birch)(Fig 2). Their growth follows the architectural model of Rauh [Hallé et al. (1978)]. This implies that the branching is rythmic, the axes are monopodial and the branches are orthotropic~~Both their architectures follow Rauh's model, meaning that the branching is rythmic, the axes monopodial and the branches orthotropic [Hallé et al. (1978)].~~ These d ~~D~~igital trees were computed with AMAPSim software [Barczi et al. (2007)]. The input of this software are architectural parameters which were provided by observations and field studies: Coudurier et al. (1993) and Heuret et al. (2006) for *Pinus pinaster*, Caraglio (1996) and Barthélémy et al. (2009) for *Prunus avium*. The choice of theses species was based on the availability of temperate species in AMAPSim database. The two trees were modelled over 50 years in open-growth conditions, which did not correspond to the same ontogenic stage

of development, but allowed both trees to be considered mature. In the final state, the pine (resp. birch) was 18,2 m (resp. 14,1 m) high. The diameter at the base was 40 cm for both species. The insertion height of the first branch was 14,3 m for pine and 4,6 m for the birch. The branches of interest were the main branches; those that were directly attached to the trunk. In addition, only branches that were more than 20 years old have been studied, so that they had a consistent loading history. Finally, 33 branches for the pine and 45 for the birch were selected. For each of the branch groups, the distributions of length L, radius r and insertion angle with the trunk θ are shown in Table 1. In this table, s_i correspond to the standard deviation of parameter i and i_m corresponds to the mean value.

Species	L_m (m)	s_L (m)	r_m (m)	s_L(cm)	θ_m (m)	s_θ (m)
Pinus pinae	5,3	0,4	5,2	0,3	70	0,01
Prunus avium	7,9	1,4	8,1	0,7	80	0,05

Table 1: Geometric distribution of branches of interest.

(a) (b)

Figure 2: AMAPSim representation of aerial architecture of 50-years old trees. (a) *Prunus avium* and (b) *Pinus pinaster* ~~50 year old birch (a) and pine (b) tree.~~

Loading scenarii: allometric laws

Each tree was composed of axes organised hierarchically according to their order: 1 for the tree seed, 2 for the trunk, 3 for the main branches, 4 for those attached to them, etc.. Each axis was described as a succession of growth units (GU), which were sections of cones, identified by a number (in order of appearance), and defined by a parent number, an order, a start and end diameter, the coordinates of the centres of both initial and final sections as well as their length (Fig 3). Note that the description provided by AmapSim did not include the internal structure of the growth units, such as eccentricity. To avoid unnecessary complications, the coordinates of the centres were taken as those of the pith. From the model data, the moments and normal forces can be computed in each growth unit, at any time of the tree's existence. In addition to a part of its own weight, each unit is subjected to the weight of its offsprings - this term referring to any growth unit that would fall if the studied one was cut. The normal

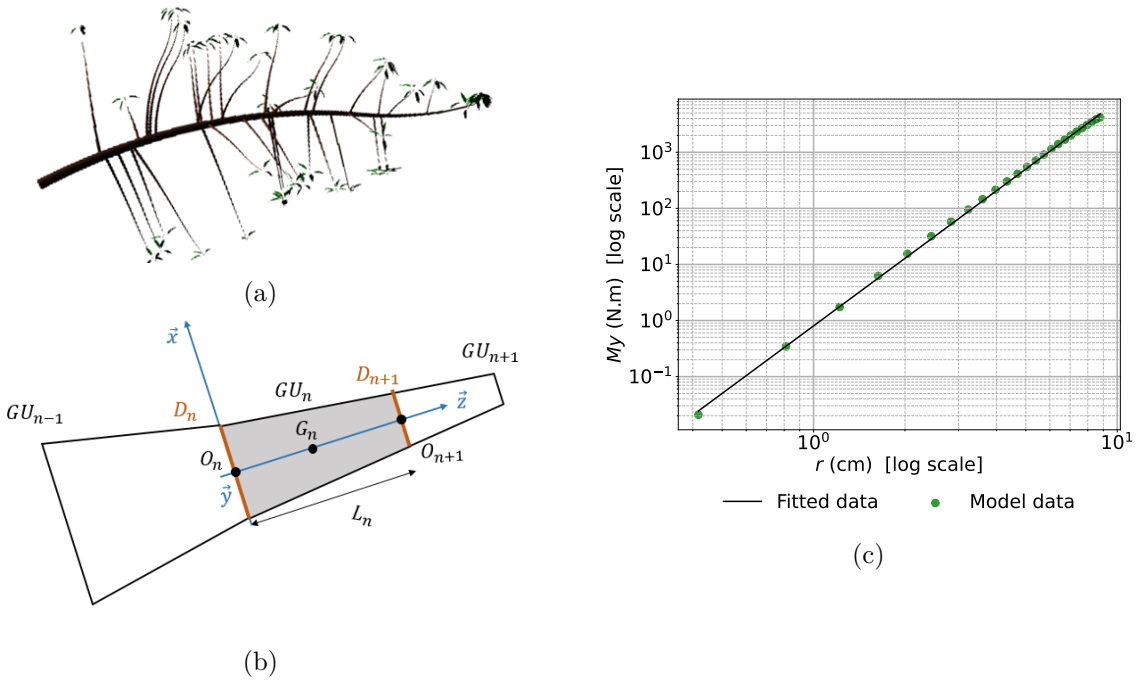

Figure 3: Allometric law of *Prunus avium*. The bending moment is calculated from the geometry of the modeled branch (a) and (b). The graph (c)~~Graph c)~~ represents the relationship between the branch diameter and the bending moment. The fitted curve provides the allometric law.

force $\overrightarrow{N_n}$ and bending moment $\overrightarrow{M_n}$ supported by the growth unit n can be written:

$$\overrightarrow{N_n} = \frac{1}{2} m_n \vec{g} + \sum_{\substack{k \succ n \\ k \ offspring}} m_k \vec{g} \tag{22}$$

$$\overrightarrow{M_n} = \overrightarrow{G_n G'_n} \wedge \left(\frac{1}{2} m_n \vec{g} \right) + \sum_{\substack{k \succ n \\ k \ children}} \overrightarrow{G_n G_k} \wedge (m_k \vec{g}) \tag{23}$$

where G_n is the centre of gravity of the current growth unit, G'_n is the centre of gravity of its second half, on the downstream side of G_n, G_k is the centre of gravity of an offspring of number $k > n$, m_i is the mass of growth unit i and $\vec{g}$ is the gravity vector. Once $\overrightarrow{N_n}$ and $\overrightarrow{M_n}$ were computed in the absolute coordinates used for the description of the whole tree, they were projected in the local coordinates system $(\vec{x'}, \vec{y'}, \vec{z})$, with $\vec{z}$ of the chosen cross section. In the following, in accordance with the development of the previous section, N_z refers to the projection of $\overrightarrow{N}$ on $\vec{z}$ and M_y to the projection of $\overrightarrow{M}$ on $\vec{y'}$.

Power law regressions were performed to recover the allometric coefficients $\lambda_M, \lambda_N, \nu_N, \nu_M$. A summary of the analysis process is proposed in Figure 3.

For the selected branch groups, t~~Branches need to have a long loading history to exhibit interesting stress profiles. Thus, only branches of order 3 (attached to the trunk) and older than 15 (resp. 17) years were selected in *Pinus pinaster* (resp. *Prunus avium*). Finally, 64 axes for pine and 65 for cherry wood were identified.T~~ he distribution of all allometric coefficients ~~for the growth unit closest to the trunk,~~ are presented in Figure 4. In *Pinus*, there was a large variation in $\nu-$coefficient, with ν_M varying by almost a factor 2 in the studied sample; indicating very variable secondary growth kinetics. In *Prunus*, the range of variation of the allometric power coefficients was smaller, which depicted a higher homogeneity of secondary growth kinetics. For both species, a great diversity in $\lambda-$ coefficients was observed, which depicted a significant variability in the loading history. This is particularly interesting as the branches

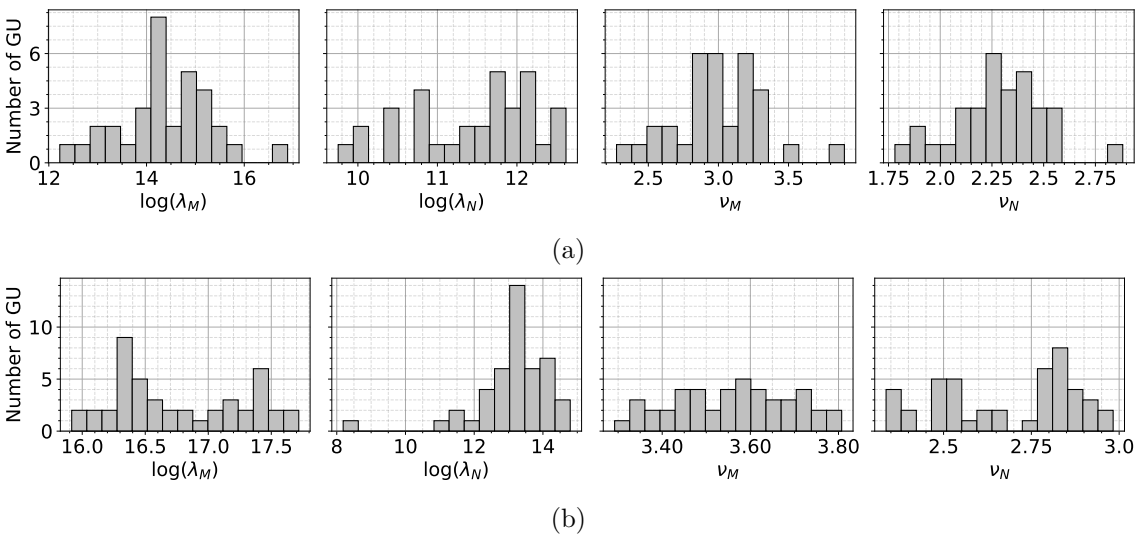

Figure 4: Statistical distribution of allometric coefficients for modelled branches: (a) *Pinus pinaster* (b) *Prunus avium* ~~(a) Pinus branches over 15 years old; (b) Prunus branches over 17 years old.~~ $\lambda_{M,N}$ refers to the weight, $\nu_{M,N}$ to the kinetic of secondary growth.

showed geometric determinants that did not vary over large ranges (Table 1). ~~For example, the radii of the axes considered in *Pinus* vary by only 1.5 cm between the smallest and largest axis, while the length varies by 20% between the shortest and longest axes.~~ Also, these coefficients do not appear to vary as a function of geometric parameters.. This reflects the complexity of predicting the loading of a branch from the determinants of the main axis, and shows the importance of branching. In both cases, these variations in the $\lambda-$coefficients result in a factor of 4 in the bending load between the lightly loaded and the heavily loaded branches.

The average values of each allometric and final geometry, indicated in table 2, will be used for the simulations.

Material data ~~and stem orientation~~

The stress values in the normal wood were fixed according to the average maturation strains advised by Thibaut and Gril (2021). Similarly, the green wood MOE were given by the correlation between dry and green MOE identified by Thibaut and Gril (2021): $Eg = 0.89 * Ed$. Dry MOE were provided by the tropix database of CIRAD [Gérard et al. (2011)]. The density of green wood was approximated by the density of water $\rho = 1000\ kg.m^{-3}$. These inputs are summarised in Table 2.
In the following section, the case of stationary growth ($\nu_b = 0$) will be considered principally and analysed thoroughly. Situations of changing curvature will be then considered briefly.

Species	λ_M	λ_N	ν_M	ν_N	r	μ_{NW}	E_d	E_g
Pinus pinae	-6.4e6	5e4	3.2	2.5	0.05	410	8.8	7.9
Prunus avium	-2.6e7	9.5e3	3.6	2.7	0.08	712	10.2	9.1

Table 2: Mean input characteristics of the branches. $\lambda_{N,M}$ and $\nu_{N,M}$ correspond to the allometric evolution of the normal load and bending moment, r (m) is the radius at the basal part of the branch, ν_{NW} (μstrain) is the maturation strain in the normal wood, and $E_{d,g}$ (GPa) is the dry and green modulus of the material.

Results

Prunus avium

Fig 5 shows simulation results obtained for *Prunus avium*, when one of the factors (eccentricity or RW) is set to zero. On Fig 5.a, the stress on the whole section is represented. In this case, the branch maintains its orientation through the formation of reaction wood only (no eccentric growth). The area near the pith is in compression (red), while the periphery is in tension (blue), with a higher tension on the upper side, allowing to maintain the orientation. Fig 5.b shows the interpolation of the stress distribution of Fig 5.a on the main axis y=0.The figure 5.c represents the maturation stress in the tension wood throughout the growth of the branch. The larger the branch grew, the higher the needed stress level. The symmetric case, with no formation of reaction wood but eccentric growth, is presented in Fig 5.d-f. This example illustrates that eccentricity alone could theoretically provide the orientation control. Fig 5.f shows the evolution of the eccentricity through the radial growth of the branch. Like the reaction wood stress in the previous case, the needed eccentricity increased when the branch grew. The pattern of stress distribution of Fig 5.d is quite similar as in Fig 5.a , with compression near the pith and tension at the periphery, but the section is off-centred and the tension at periphery is the same all around the section, confirming the absence of reaction wood.

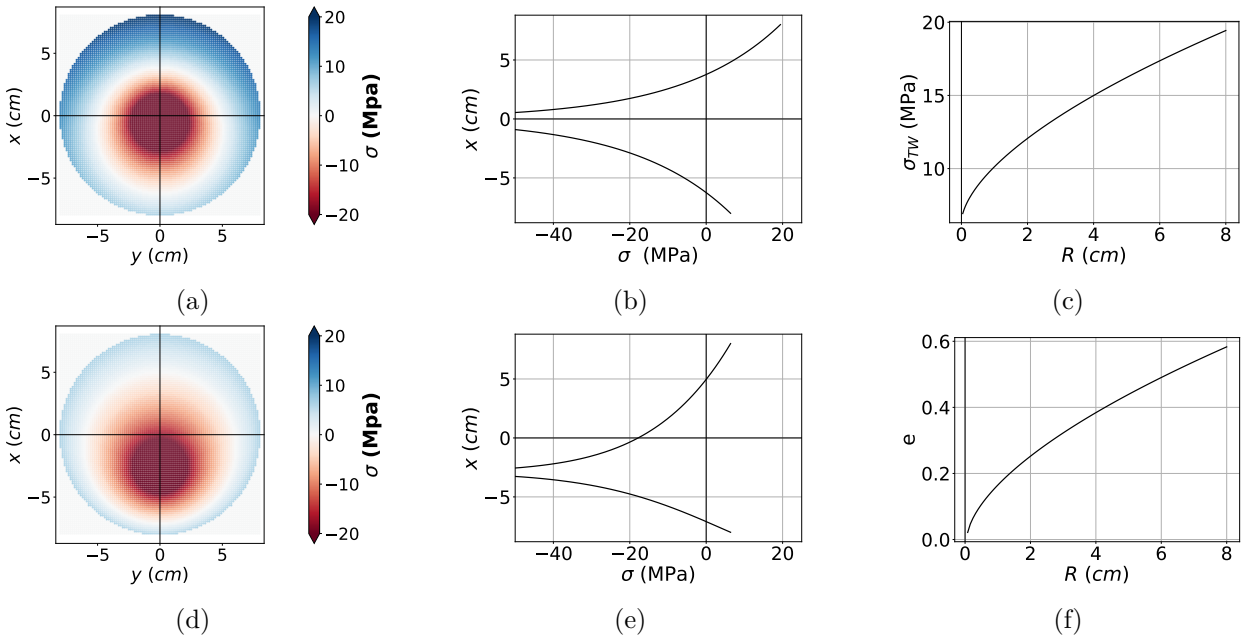

Figure 5: *Prunus avium*: The horizontal orientation of the branch is maintained by the two different processes ~~drivers~~: (a-c) the maturation stress provided by the formation of reaction wood; (d-f) the eccentric growth; (a,d) 2D visualisation of the growth stress in the whole section; (b,e) Growth stress profile on diameter y=0. (c,f) Parametric representation of the tropic driver, maturation stress (c) and eccentricity (f).

~~Several postural control scenarii have been computed. First, the ability of the branch to maintain its orientation through RW formation only (Fig 5.a-c) or secondary growth eccentricity only (Fig 5.d-f) is evaluated. Then, combinations of these options is proposed (Fig 6): for each combination, one parameter (growth eccentricity or maturation) is assumed to be uniform throughout the growth of the branch, while the other is assumed to be the driver of orientation control.~~

Fig 6 shows the combination of the two factors. For each of them, three different scenarii were proposed. In Fig 6.a, the reaction wood factor controlled the orientation. Different eccentricities, ranging from -0.5

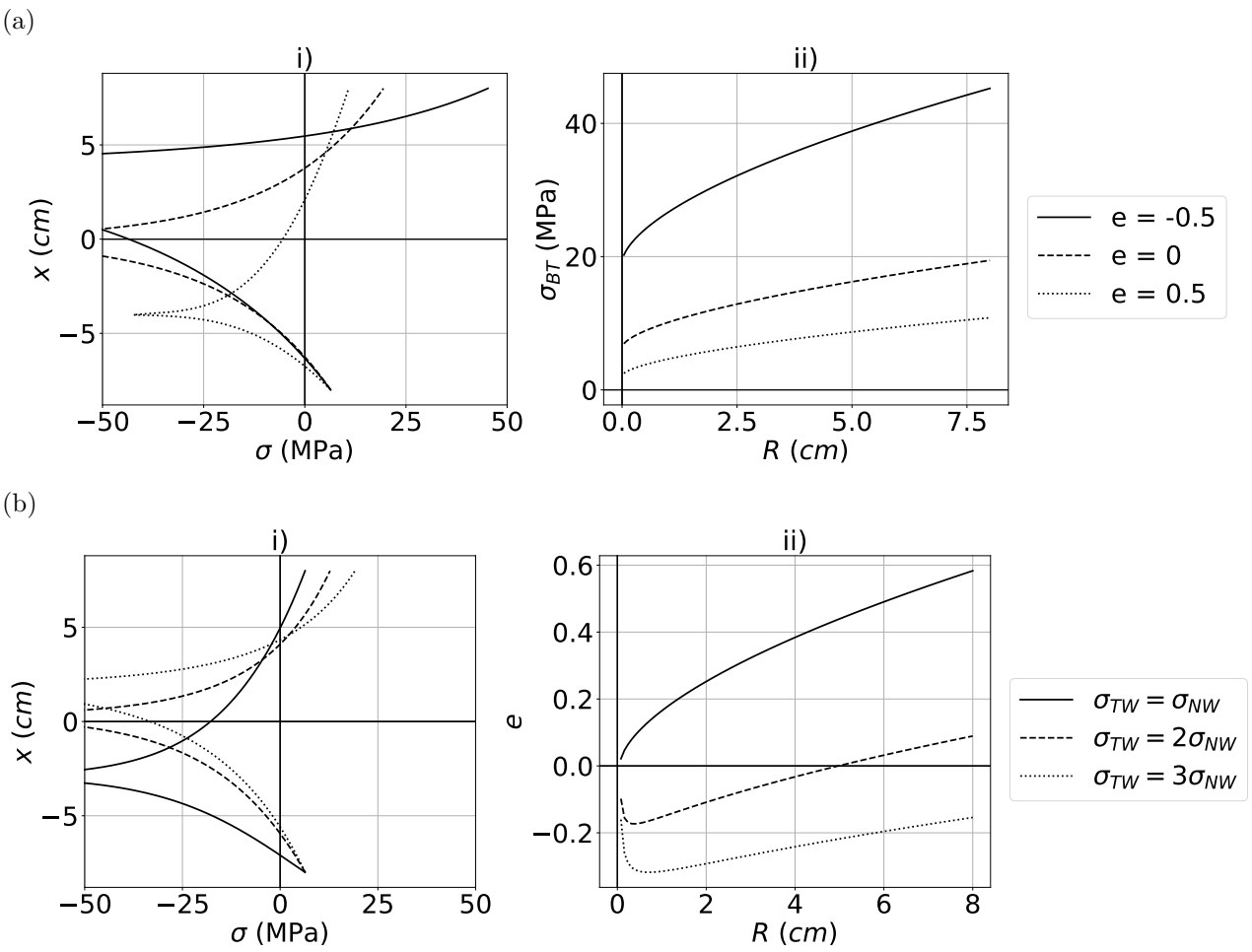

Figure 6: Different possible options to maintain the orientation of *Prunus avium* branches: (a) a constant eccentricity combined with the maturation that becomes the main driver of postural control; or (b) a constant maturation gradient combined with an eccentricity that becomes the main driver of postural control.~~Illustration of different straightening strategies for *Prunus avium*: (a) constant eccentricity, the maturation is the main driver of postural control; (b)constant difference of maturation stress, the eccentricity is the main driver of postural control.~~

to 0.5 were imposed. The resulting stress patterns are represented in Fig 6.a.i : the higher tension on the upper side maintained the posture. The more hypotrophic the eccentricity, the higher the tension stress at periphery. This is confirmed by the evolution of reaction wood maturation stress through branch growth in Fig 6.a.ii. The situations where the eccentricity controlled the posture are shown in Fig. 6.b. Where uniform tension was imposed ($\sigma_{TW} = 2\sigma_{NW}$,$\sigma_{TW} = 3\sigma_{NW}$), the eccentricity pattern became particular: we observed a decrease during the first year, followed by an increase (Fig 6.b.ii). This is explained by the growth scenario: at the beginning of the development, fixing a uniform reaction wood formation tended to right-up the stem, while a stationary orientation was imposed. Therefore, the eccentricity process counteracted this righting up movement, leading to the initial decrease. As the branch grew, the effect of the reaction wood decreased and the branch tended to bend forward: the eccentricity counteracted this trend, leading to the final increase. This coordination problem may probably be specific to our scenario that imposed a stationary orientation throughout the entire growth the branch, including the first stages of development.

Pinus pinaster

For *Pinus pinaster*, we used the same approach. The set of results is presented in Fig.7 and Fig.8. When no eccentricity was involved (Fig 7.a-c), a light compression stress was observed on the lower side of the section. When the branch grew, the compression stress increased (Fig 7.c). In case of no reaction wood formation (i.e. no maturation stress), the distributions of growth stress and eccentricity (7.d-f) were quiet similar to the previous example with the birch tree: tension in periphery, compression near the pith, and an increasing eccentricity with branch growth.

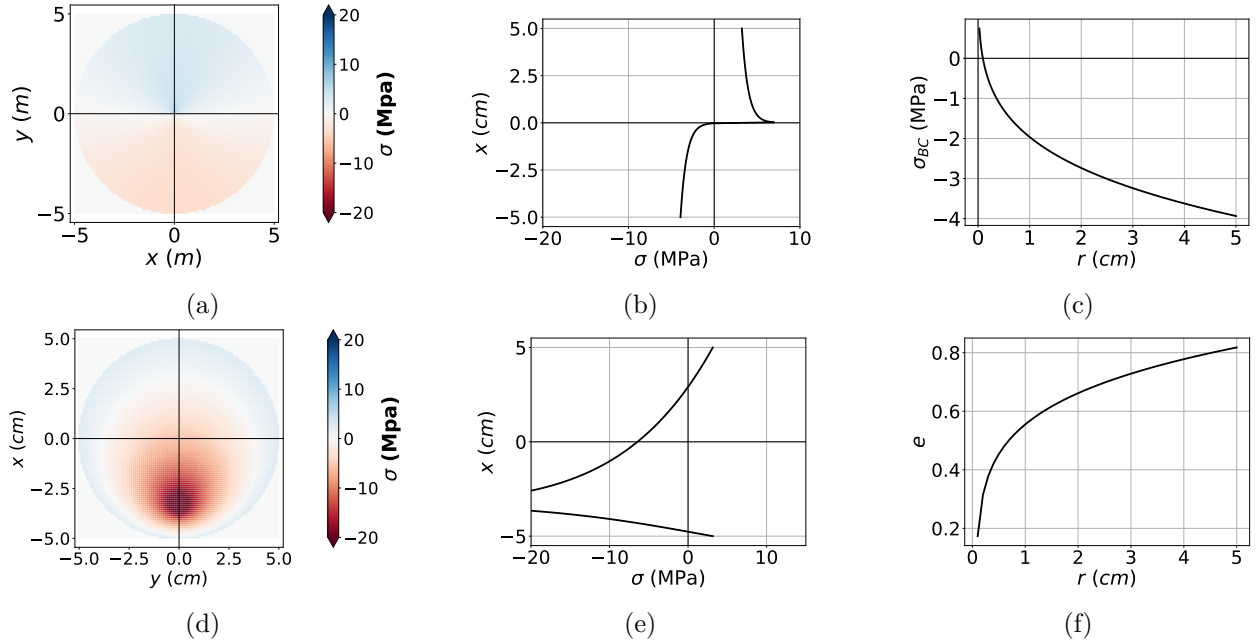

Figure 7: *Pinus pinaster*: Horizontal orientation maintained by the two different processes ~~drivers~~: a-c) maturation stress and d-f) eccentricity. Different types of representation are proposed: a) (resp. d)) 2D visualisation of the growth stress (resp. eccentricity) in the whole section. b) and e) Growth stress profile on the line y=0. c) and f) Parametric representation of the tropic driver: maturation stress and eccentricity.

The combination of the two factors is shown in Fig. 8. As for *Prunus avium*, different eccentricities were imposed (Fig.8.a): the more epitrophic the eccentricity, the higher reaction wood maturation stress. Although the different compression stress levels were close, the dynamic of this stress within the growth of the branch was different (Fig 8.a.ii). Also, the stress pattern exhibits a difference near the pith (Fig. 8.a.i), with some tension in this area for eccentricity $e = 0.5$. in case of a uniform reaction wood maturation (8.b), the profile remained quite similar to birch tree. We could not impose a too low compression stress because of the above-mentioned coordination incompatibility.

Influence of branch orientation: the stationarity hypothesis

In order to evaluate the relevance of the stationarity hypothesis i.e. the branch keeps the same orientation), different growth scenarii are considered. For each branch, the case of active up-righting ~~straightening~~ or passive bending was modelled (using the equation 17). Passive bending was driven by increasing weight, calculated on the modelled branches. Up-righting was driven by the maturation gradient, which was set at 400 μstrain ($\sigma \approx 3.2$ MPa) for pine and 700 μstrain ($\sigma \approx 6.2$ MPa) for birch (the gradient was of the order of magnitude of NW stress). The results are shown in Figure 9. In birch, no major change of the stress pattern was observed. In contrast, the pattern changed greatly for pine. For a passive-bending

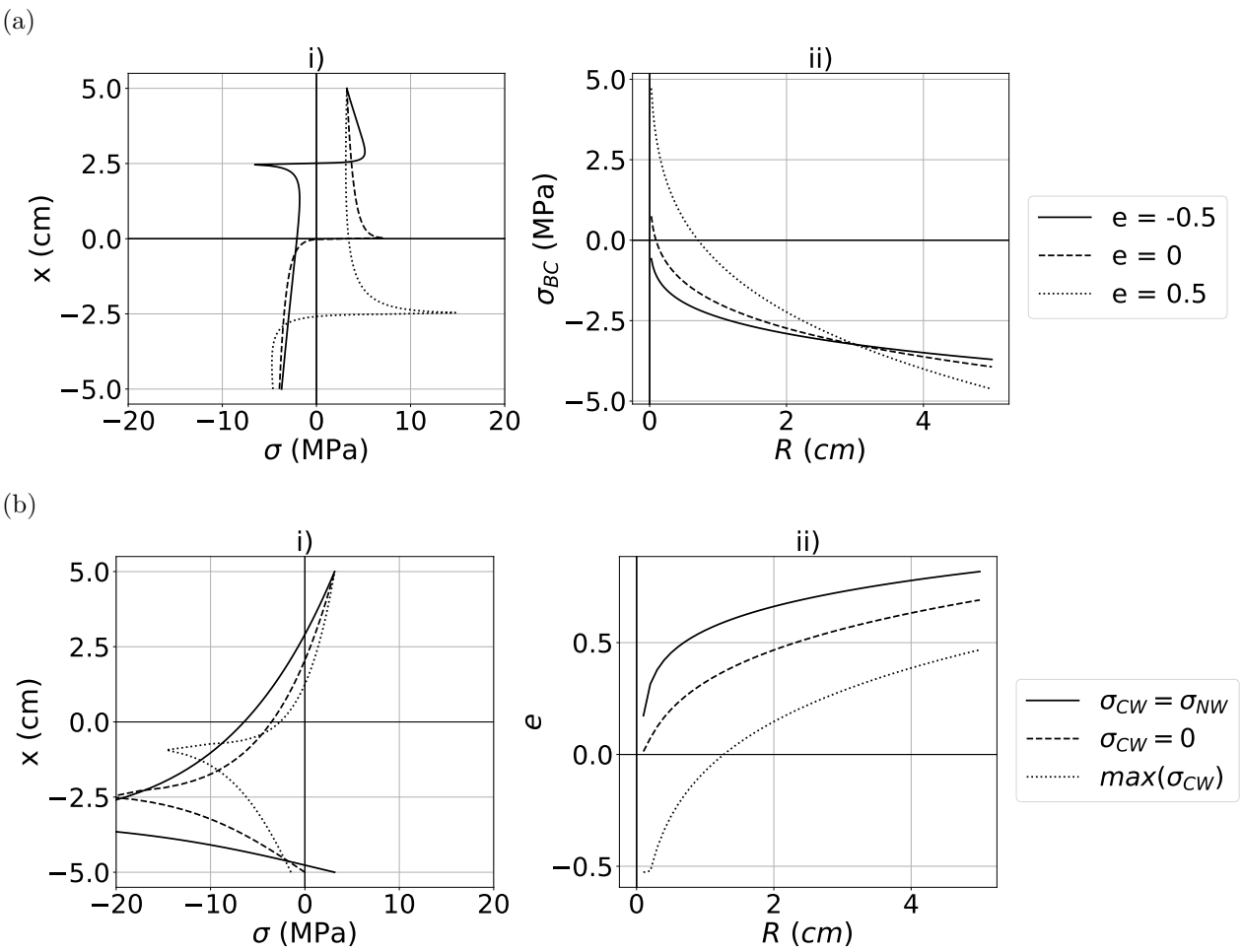

Figure 8: Different options to maintain the orientation for *Pinus pinaster* branches: ~~Illustration of different straightening strategies for *Pinus pinaster*:~~ (a) constant eccentricity, the maturation is the main driver of postural control; (b): constant maturation gradient, the eccentricity is the main driver of postural control.

branch, a 'V' profile and the absence of compression wood were observed. For up-righting ~~straightening~~, the previously-mentioned profile with tension at the pith was observed.

Discussion

Prunus avium: heavily loaded hardwood

Regarding the stress distribution (Fig.5), using either eccentric growth or reaction wood led to realistic orders of magnitude (except near the pith, which is an intrinsic limit of our model. This specific point is discussed in section *Limits of the model*). In the case with no eccentricity, a tensile strain of $\mu_{RW} \approx 2140\mu$strain ($\sigma_{TW} \approx 19.5$ MPa) was obtained, quite similar to literature values, for much smaller branches: on 4 cm plagiotropic branches of eight tree species, Tsai et al. (2012) reported an average strain in reaction wood of around 2100μstrain, with some values up to $\approx 5000\mu$strain. When combined with uniform eccentricity, it seems safer to promote the growth on the upper side: it minimises both high tensile stress and area with high compression stress. Interestingly, the worst case (hypotrophic eccentricity $e = -0,5$, more, solid line in Fig 6.a) led to levels approaching the limits, but already observed [Huang et al. (2005); Huang et al. (2012)]: $\mu_{RW} \approx 4970\mu$strain ($\sigma_{TW} \approx 45.4$ MPa). Note that

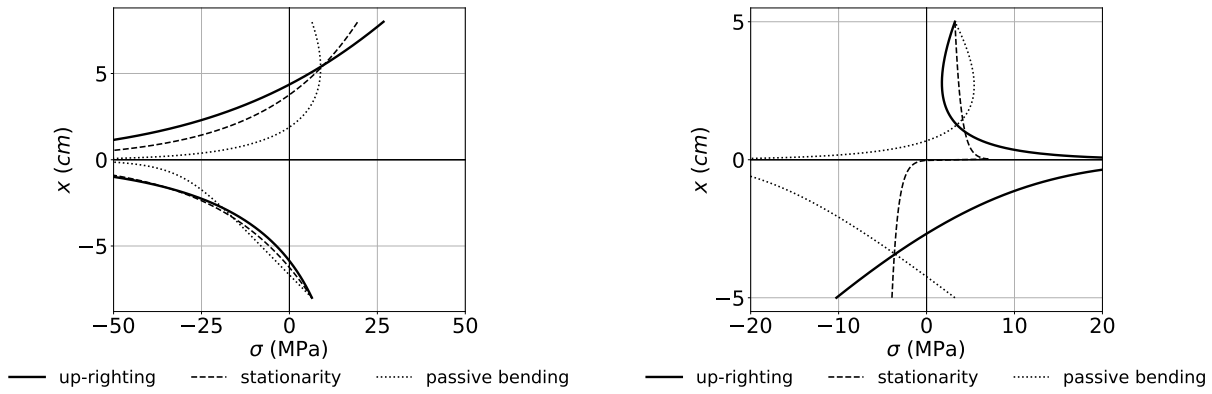

(a) Prunus (b) Pinus

Figure 9: Distribution of growth stresses for different orientation scenarios.

although for softwoods, there is a consensus on the usually observed eccentricity orientation (hypotrophic) [Timell (1986)], the eccentricity has been observed in both directions in hardwood branches [Kucera and Philipson (197 although not usually in trunk. Therefore, this could be a tropic response for angiosperms branches, that tend to bend forward. This non-optimal pattern would be the consequence of a coordination between eccentricity and maturation stress. An extensive measurement campaign on branches would be needed to clarify this point. In the absence of RW (Fig 5.d-f), the eccentricity alone ensured the orientation. The maximal value was around 0.6, which seems quite high compared to literature values. For example, Hung et al. (2017) performed measurements on 10 plagiotropic branches of *Koelreuteria henryi*. The average radius was 2.6 cm, and the eccentricity had an average value of -0.37, with a maximum at -0.54. Unpublished data on more than 150 branches from six different temperate species showed very different patterns, depending from the species, but eccentricity was never below -0.5. This suggests that eccentricity is a limited driver of postural control. This result is in line with the work of Alméras et al. (2005), who showed that eccentricity in leaning stem explains a much lower part of the curvature than the maturation gradient ($\approx 29\%$ for eccentricity while $\approx 66\%$ for maturation gradient).

The combination of radial growth eccentricity with uniform maturation stress showed the same tendency as the dual combination (uniform eccentricity): a higher maturation stress led to a larger eccentricity. Comparing all simulations, the most optimal case was a constant positive eccentricity (dotted line in Fig 6.a). However, experimental observation showed that this is not the usual configuration for branches. It raises interesting question on the main mechanical driver of branch construction. From a biological point a view, it could be more "costless" to produce TW than eccentricity, but this hypothesis was not yet investigated. Also, more work is needed to understand how TW and eccentricity are linked in angiosperm trees: since they may have some uncoordinated action, we can wonder if they have common triggered factors.~~Both strategies alone (Fig.5) lead to realistic orders of magnitude (except near the pith, which is an intrinsic limit of our model; this specific point is discussed in section *Limits of the model*). Across the chosen combinations, no single strategy seems to be more efficient than the other. For example, eccentricity alone (5.a-c and 6.b, solid line) may be sufficient to maintain the branch orientation while keeping a sufficient mechanical safety margin ($\max(e) = 0.6$). In comparison, with zero eccentricity (Fig.6.a, dashed line), TW alone leads to a tensile strain $\mu_{RW} \approx 2140\mu$strain ($\sigma_{TW} \approx 19.5$ MPa), also far from limits observed in literature [Huang et al. (2005); Huang et al. (2021)]. Moreover, eccentricity and deformation in TW acts as an optimisation of branch control and resistance to breakage: promoting epitrophic eccentricity (more radial growth on the upper side) allows less tension in TW: the more space eccentricity leaves to TW, the lower the stress in it. Interestingly, the worst case (hypotrophic eccentricity, more radial growth on the lower side, solid line in Fig 6.a) leads to orders of magnitude that are on the border of limits, but observable: $\mu_{RW} \approx 4970\mu$strain ($\sigma_{TW} \approx 45.4$ MPa). Note that although for softwoods, there is~~

~~a consensus on the eccentricity orientation (hypotrophic) for tropism responses [Timell (1986)], hardwood species can show eccentricities in both directions [Kucera and Philipson (1977); Kucera and Philipson (2009b); Kucera~~
~~The hypotrophic eccentricity (Fig 6.a) is obviously not motivated by an optimisation of postural control, suggesting the existence of trade-offs with other vital functions.~~
~~Even if the observation is the same (epitrophic eccentricity lead to less intense TW), graphs 6.b (dashed and dotted lines) show profiles that have higher safety margins than those in Figure 6.a. When combined, it seems more efficient to vary the eccentricity and keep a constant difference of maturation stress than to keep a uniform eccentricity and to vary the maturation stress. To date, there is no study that has attempted to investigate the variations in space and time of the eccentricity in the branches. This is a very interesting perspective to understand the interaction between eccentricity, maturation and postural control of inclined axes.~~

***Pinus pinaster*: lightly loaded softwood**

First of all, the values of the stress distribution were much lower than for *Prunus avium.* This was explained by the size of the modelled branches: the average bending moment is much higher for birch tree than for pine, by a factor roughly 10 (see λ_M and λ_N in Table 2). The effect of each factor alone (Fig 7) suggested that maturation is a much more efficient option than eccentricity. To ensure the same growth scenario, the eccentricity alone rose to about 0.8, which is close to a theoretical limit, whereas maturation alone led to low maturation strains in CW (<500 μstrain, corresponding to 4 MPa). Besides, this eccentricity was not in the direction of what is commonly observed. This point remains logical, because without CW, the epitrophic eccentricity is the only way to counteract the effect of gravity.
A uniform eccentricity combined with RW formation led to quite similar patterns (Fig 8.a): for this range of loading, the eccentricity had little influence on stress distribution.Considering that the density of elastic energy is proportional to the square of the stress, the pattern produced a low level of stored elastic energy, possibly reducing the risk of mechanical failure. Also, although eccentricity did not bring much variations in the value of the maturation stress, it considerably modified the shape of the resulting stress profiles (Fig 8.a.i). Indeed, these profiles can become 'crenellated' (Fig 8.a.i, dashed curve for zero eccentricity, solid curve for $e = -0.5$) or include tension at the pith (dotted line for $e = 0.5$). It seems that before producing tension in the pith, an efficient configuration could be reached by generating compression below the pith and tension above. Ideally, this may be a very relevant option for branches. These results about the mechanical strategies of branches should be confronted to experimental measurements. Otherwise, these pattern changes could also be an optimisation of the residual strength of wood: CW is known to have high compressive strength conferred by its high lignin content and cell wall structure. Generating some tension at the pith allows the branch to create more CW. To answer this question it would be necessary to take into account strength parameters in our stress computation model. Adding a damage-elastoplastic law would also allow to study the effects of stress relaxation and to observe if some profiles, that are here not optimal for maintaining the branch orientation, could possibly become optimal for resisting breakage.
Using eccentricity combined to RW formation (Fig 8.b) leads to usual patterns, with compression near the pith, tension on the upper side and compression on the lower one. Eccentricity is epitrophic: this is the opposite to what is usually observed: unpublished data on 20 branches (average radius of 3 cm) of *Pinus nigra* showed an average eccentricity of -0.2. This non-intuitive result is partly explained by our hypothesis of uniform stiffness, as will be discussed later.It is also explained here by the change of sign between NW and CW. In the early stages of growth, as long as the stress in the CW is lower than in the NW, the best option to maintain the orientation is to do epitrophic eccentricity. Once the stress in the CW becomes higher than in the NW, it is more efficient to do hypotrophic eccentricity. Our scenarios do not allow us to reach stress levels in compression that are higher than the stress in normal wood. This is due to the above mentioned incompatibility of our scenario.

~~Similarly, for *Pinus pinaster*, we compare the ability of maturation process alone (Fig 7.a-c) and growth eccentricity alone (Fig 7.d-f) to maintain a constant orientation, then study the combination of these~~

processes (Figure 8). Note that the average bending moment due to weight is much higher for birch tree, by a factor roughly 10, than for pine (see λ_M and λ_N in Table 2). This may explain why the straightening drivers are much less triggered in the case of this pine. Moreover, in the current model the Young's modulus is supposed to be uniform in the whole cross section. While this hypothesis does not have much impact on the stress profiles for hardwoods, where both TW and NW produce tensile stress and the difference of Young's moduli is moderate, it modifies the results for softwoods much more. Indeed, although CW of softwoods is typically denser than NW, due to the higher inclination of cellulose microfibrils, its Young's modulus is often much lower. This explains for a part the commonly observed association of CW production with eccentric growth. This is an important limitation of the proposed formulation and will have to be kept in mind when discussing the results. The analysis of each strategy alone (maturation: Fig 7.a-c and Fig.8.a dashed line; eccentricity: Fig 7.d-f and Fig.8.b solid line) suggests that maturation is more efficient than eccentricity. To ensure the same growth scenario, the eccentricity alone rises to about 0.8, which is not far from a limit value, whereas maturation alone leads to low maturation strains in CW (<500 μstrain, corresponding to 4 MPa). Besides, this eccentricity is not in the direction of what is commonly observed. This point remains logical, because without CW, the epitrophic eccentricity leads to shifting the bending centre upward to limit the bending moment load. Finding an eccentricity opposite to the usual one observed is therefore quite plausible. In fact, the eccentricity in the early stages of development generates a coordination problem, especially for softwoods. For hardwoods, the simultaneous building of TW and eccentricity is not an issue, whereas building a hypotrophic growth pattern without CW is not efficient for softwoods.In case of combined effects, although eccentricity alone ensures stationarity, it does not succeed anymore when combined to a uniform maturation (red dotted line in Fig. 8.b). For the chosen parameters, this means that if the maturation strain was higher than -180 μstrain ($\sigma_{CW} \approx 1.4$ MPa, black dotted line in Fig. 8.b) the branch could not ensure its orientation using the eccentricity process only. As said before, the early stages of development in softwood seems to generate coordination problem. Finally, varying the eccentricity while keeping the maturation stress constant seems to be an irrelevant biomechanical strategy for the branch. Beyond this result, one can also wonder if this case was realistic: to what extent are there constant maturation constraints throughout the growth of the branches? But if these situations do really exist, then eccentricity clearly does not have a crucial role in maintaining postural control. For the other combined effects, the eccentricity does not bring much change in the value of the maturation stress (Fig. 8.a). However, it considerably modifies the shape of the resulting stress profiles (Fig.8.a.i). Indeed, these profiles can become 'crenellated' (Fig.8.a.i, dashed curve for zero eccentricity, solide curve for $e = -0.5$) or include tension at the pith (dotted line for $e = 0.5$). These two particular patterns are represented in the whole section in Fig. **??**. It seems that before producing tension at the pith, an optimal configuration can be reached by generating compression below the pith and tension above. Ideally, this may be what each branch should tend to do. These results about the branches mechanical strategies should be compared with experimental measurements. Otherwise, theses changes of patterns could also be an optimisation of the residual strength of wood: CW is known to have better compressive strength conferred by its high lignin content and cell wall structure. Generating some tension at the pith allows the branch to create more CW. To answer this question correctly, it would be necessary to build a fracture model and to include it to our stress computation model. For example, adding an damage-elastoplastic law would allow to study the effects of stress relaxation and to understand how some profiles that are not optimal for straightening can possibly be optimal for resisting breakage.

Influence of the branch's orientation : the stationary hypothesis

In order to evaluate the relevance of the stationarity hypothesis, different growth scenarios are considered. For each branch, the case of active up-righting straightening or passive bending is modelled. Passive bending is driven by increasing weight. Up-righting is driven by the maturation gradient, which is set at 400 μstrain ($\sigma \approx 3.2$ MPa)for pine and 700 μstrain ($\sigma \approx 6.2$ MPa) for birch tree (the gradient is of the order of magnitude of NW stress). The results are shown in Figure 9. In birch, no major change of the

~~stress pattern is observed. In contrast, the pattern changes greatly for pine. For a passive-bending branch, a 'V' profile and the absence of CW are observed . For up-righting straightening, the previously-mentioned profile with tension at the pith is observed.~~ In both trees, the orders of magnitude are compatible with a mechanical safety margin for the branches. Apart from modified tropisms (change of light environment, weight change by loss of part of the branch, etc.), the maintaining of the orientation is quite common for real branches. However our simulations suggest that if, for any reason, they need to modify their orientation, they can do it without taking too much mechanical risk. The hypothesis of branch direction stationarity is totally in accordance with the long-term mechanical requirements needed during the construction ~~building~~ of branches.

Vertical bending moment vs horizontal bending and torsion moments

One of the hypothesis of our model was that the vertical bending moment (M_y) prevails over the torsional M_z and horizontal bending M_x moments. This allowed to consider only one direction of eccentricity and to avoid all the non-linear terms generated by the torsional components. We evaluated the maximum values of the three moments for all modelled branches of each species for comparison purpose. The results are presented in figure 10. They enlighten that for every comparison, the vertical moment shows much higher values than the torsional and horizontal bending moments and validates our initial hypothesis.

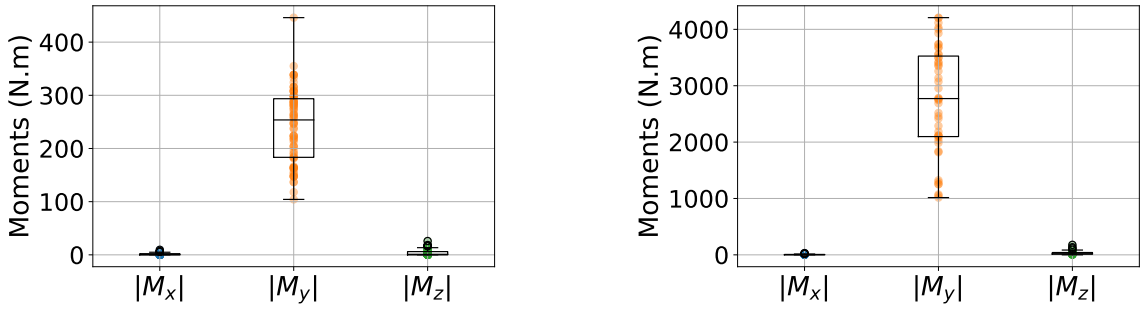

(a) Pinus (b) Prunus

Figure 10: Comparison of maximum moments for modeled branches. Mx: horizontal moment; My: vertical moment; Mz: torsional moment.

Limits of the model

The hypothesis of homogeneous wood stiffness in the whole section is questionable. Systematic stiffness differences have been observed between wood types (TW or CW vs NW). Alméras et al. (2005) have studied the variation of Young's modulus in the section of leaning stems from 14 angiosperms and 3 gymnosperms, all coming from different families. For the angiosperms, the average Young's modulus of TW was higher than in NW by 15%, while for the gymnosperms, the Young's modulus was 38% lower in CW than in NW. This heterogeneity of rigidity plays a role in the postural control of the stems [Alméras et al. (2005); Alméras et al. (2010); Alméras et al. (2017)]. In our case, either a higher rigidity in TW or a lower in CW would make the branch bend upward. In the current formulation of the model imposing an homogeneous stiffness, an almost equivalent effect would have been obtained by an initial offset in the eccentricity. Calling this offset tentatively 'compensating eccentricity' e_c (Fig 11), the model computed a total eccentricity, e, combining e_c and the "real" eccentricity needed to maintain the orientation. Therefore, in case in RW formation on one side, the eccentricity displayed need to be offset by e_c to correspond to more realistic situations. This explains, for instance, why the simulations for the softwood resulted in hypertrophic eccentricity while it is well-known that inclined softwood stems usually exhibit hypotropic eccentricity. Although data are missing to approximate the value of this parameter, and further work is needed to assess theoretically the possible equivalence between rigidity variations and

eccentricity, the available information on relative stiffness of NW and RW suggests a more important effect in gymnosperms than in angiosperms.

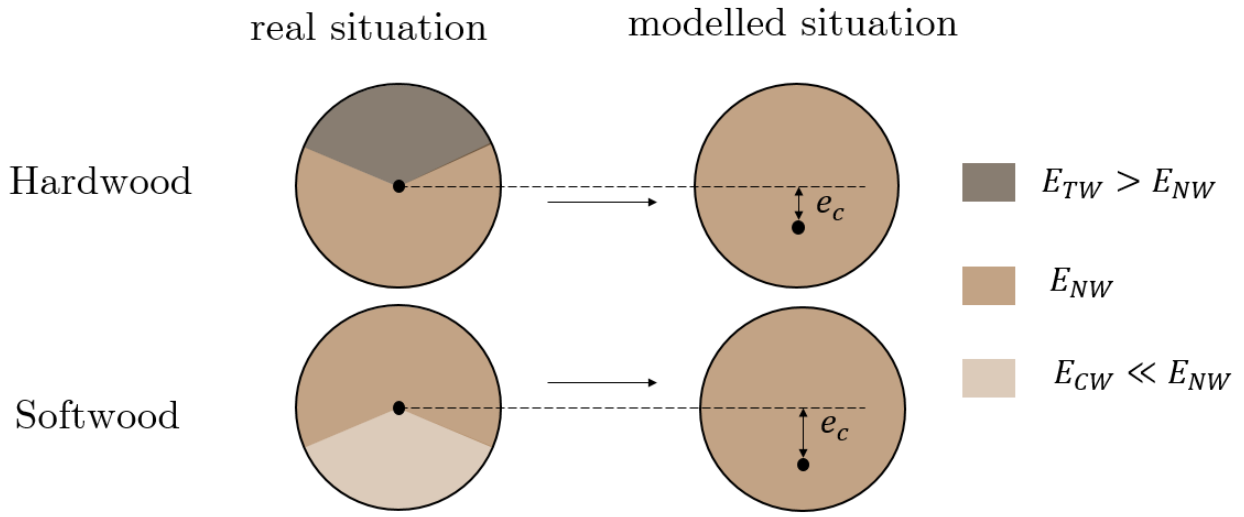

Figure 11: How the hypothesis of a uniform wood stiffness impacts the initial position of the pith.

The evaluation of the stress during the first stages of branch's development is an issue of the model. In almost every stress profiles, a tension or compression peak is generated in the pith. It generally exceed the wood strength, which is not compatible with branch sustainability. This point could be corrected in two ways. First, the role of the bark could be taken into account. Its mechanical role for small axes has already been studied and its importance in postural maintain ~~straightening~~ was clearly highlighted [Clair et al. (2019); Ghislain et al. (2019)]. Our model could include the mechanical action of bark in the early stages of branch development. This improvement would require additional data about the mechanical behaviour of the bark but would bring more realistic stress predictions and limit the artefacts at the pith. A second exciting perspective would be to take into account the elastoplastic behaviour of wood. By imposing a realistic plastic strain limit, the peak at the pith would then disappear; and the increments would be spread over the middle part of the section, thus modifying the non-realistic patterns previously observed.

~~A another limit is the hypothesis about wood stiffness. It is particularly unfavourable for softwoods, because it reinforces some geometric phenomena (see the one in Fig.8.a.i). In this context, it would be very interesting to evaluate the potential link between eccentricity and modulus variations. If the latter is established, the eccentricity that we would impose with the model would serve to compensate or amplify the effect of the tension wood. However, it remains unclear whether or not this would explain the limited action available to the branch in the case of a constant maturation stress.~~

Finally, modelling the evolution of normal force and bending moment loads by allometric laws was not optimal. Indeed, the orientation of the branch may vary with time, which implies variations of the effect of weight. For example, modelling a constant increase of the normal force is inappropriate if the inclination of the branch decreases with time. An improvement of our model could be the construction of loads based on equivalent length allometries taking into account the mass of the branch, and the computation of the loads for each position in the right reference frame.

Conclusion and perspectives

A semi-analytical growth stress model has been developed a in the context of branch development. At each radius increment, the stress balance is computed in order to fit with a fixed curvature. A first novelty

of this model is that it takes into account the role of the eccentricity variation over the years. A second contribution is that the model computes the stress distribution in the whole cross-section. We tested the effectiveness of two well-known biomechanical processes ~~strategies~~ of woody plants to control the orientation of their axes: the eccentric radial growth ~~secondary growth eccentricity~~ and the formation of reaction wood. The case of one softwood *Pinus pinaster* and one hardwood *Prunus avium* ~~branches~~ were computed using data provided by AMAPSim software. both trees~~hardwood~~, growth stress simulations showed that maturation stress was more efficient than eccentric radial growth~~both strategies are efficient~~ to maintain a fixed orientation, (i.e. to counter the increasing gravity constrain applied to the growing branch). For the hardwood branches, the computations highlited that the eccentricity needed to maintain orientation did not corroborate the observations reported~~i~~n literature. This suggests that this parameter probably provides another function than the orientation control, like, for instance, the improved bending strength of the branch that provides it a greater mechanical safety.~~On the contrary, in the case of softwood , reaction wood formation appear to be more efficient than eccentric growth. Obviously, in all cases, the combination of both processes yields very high stress levels that are able to keep the branch straight or modify its orientation. Our model also enlightened that few strategies, such as forming reaction wood uniformly over time while allowing eccentric growth, are not optimal to maintain the orientation.~~. For the softwood branches, although the model showed that eccentric radial growth did not play a major role in maintaining the branch's orientation, it does modify the shape of the stress profiles in the cross section of the branch.~~However, since growth eccentricity does not play a major role in straightening capabilities, it does not influence much the shape of the stress profiles~~. A few odd and critical profiles, crenelated or with tension near the pith, have been identified. Their analysis provided exciting perspectives for further experimental works in order to get real data. ~~Finally, for lightly loaded softwood branches, the eccentric growth plays a minor role in straightening~~.

Now that a complete model is available, it becomes crucial to start experimental investigations on branches in order to compare the outputs with real in situ observations. Especially, we need to evaluate the relevance of the different biological processes used by branches in order to ensure their mechanical sustainability over the years.

From a biological point of view, a key point for understanding branch sizing is the question of biomass costs. Building additional wood on one side or forming reaction wood are carbon sinks with possible trade-offs. In order to investigate this point, our model could help by affecting a cost to the production of reaction wood as well as to eccentric growth. The resulting computations could then help to understand the relevance of some options ~~strategies~~ and would lead to coupling the biomechanical point of view to other biological considerations.

References

T. Alméras, D. Jullien, and J. Gril. *Modelling, Evaluation and Biomechanical Consequences of Growth Stress Profiles Inside Tree Stems*, pages 21–48. Springer International Publishing, Cham, 2018. ISBN 978-3-319-79099-2. doi: 10.1007/978-3-319-79099-2_2. URL `https://doi.org/10.1007/978-3-319-79099-2_2`.

T. Alméras and B. Clair. Critical review on the mechanisms of maturation stress generation in trees. *Journal of The Royal Society Interface*, 13(122):20160550, 2016. doi: 10.1098/rsif.2016.0550. URL `https://royalsocietypublishing.org/doi/abs/10.1098/rsif.2016.0550`.

T. Alméras and M. Fournier. Biomechanical design and long-term stability of trees: Morphological and wood traits involved in the balance between weight increase and the gravitropic reaction. *Journal of Theoretical Biology*, 256(3):370–381, 2009. ISSN 0022-5193. URL `http://www.sciencedirect.com/science/article/pii/S0022519308005389`.

T. Alméras, A. Thibaut, and J. Gril. Effect of circumferential heterogeneity of wood maturation strain,

modulus of elasticity and radial growth on the regulation of stem orientation in trees. *Trees*, 19(4): 457–467, 2005. ISSN 1432-2285. URL https://doi.org/10.1007/s00468-005-0407-6.

P. Ancelin, T. Fourcaud, and P. Lac. Modelling the biomechanical behaviour of growing trees at the forest stand scale. part i: Development of an incremental transfer matrix method and application to simplified tree structures. *Annals of Forest Science*, 61(3):263–275, 2004.

R. R. Archer. On the distribution of tree growth stresses. ii. stresses due to asymmetric growth strains. *Wood Science and Technology*, V10:293–309, 1976.

R. R. Archer and F. E. Byrnes. On the distribution of tree growth stresses – part i: An anisotropic plane strain theory. *Wood Science and Technology*, 8(3):184–196, 1974. ISSN 1432-5225. URL https://doi.org/10.1007/BF00352022.

J.-F. Barczi, H. Rey, Y. Caraglio, P. de Reffye, D. Barthélémy, Q. X. Dong, and T. Fourcaud. AmapSim: A Structural Whole-plant Simulator Based on Botanical Knowledge and Designed to Host External Functional Models. *Annals of Botany*, 101(8):1125–1138, 09 2007. ISSN 0305-7364. doi: 10.1093/aob/mcm194. URL https://doi.org/10.1093/aob/mcm194.

D. Barthélémy, Y. Caraglio, and S. Sabatier. 4.1 crown architecture of valuable broadleaved species. *Valuable broadleaved forests in Europe*, 22:87, 2009.

D. Barthélémy and Y. Caraglio. Plant Architecture: A Dynamic, Multilevel and Comprehensive Approach to Plant Form, Structure and Ontogeny. *Annals of Botany*, 99(3):375–407, 01 2007. ISSN 0305-7364. doi: 10.1093/aob/mcl260. URL https://doi.org/10.1093/aob/mcl260.

Y. Caraglio. Le développement architectural du merisier. *Forêt Entreprise 107*, (107):72–80, 1996.

B. Clair, B. Ghislain, J. Prunier, R. Lehnebach, J. Beauchêne, and T. Alméras. Mechanical contribution of secondary phloem to postural control in trees: the bark side of the force. *New Phytologist*, 221(1): 209–217, 2019. doi: https://doi.org/10.1111/nph.15375. URL https://nph.onlinelibrary.wiley.com/doi/abs/10.1111/nph.15375.

T. Coudurier, D. Barthelemy, B. Chanson, F. Courdier, and C. Loup. Premier résultats sur la modélisation du pin maritime pinus pinaster ait.(pinecae). *Architecture des arbres fruitiers et forestiers*, page 306, 1993.

C. Coutand, M. Fournier, and B. Moulia. The gravitropic response of poplar trunks: Key roles of prestressed wood regulation and the relative kinetics of cambial growth versus wood maturation. *Plant Physiology*, 144(2):1166–1180, 2007. ISSN 0032-0889. doi: 10.1104/pp.106.088153. URL http://www.plantphysiol.org/content/144/2/1166.

J. B. Fisher and J. W. Stevenson. Occurrence of reaction wood in branches of dicotyledons and its role in tree architecture. *Botanical Gazette*, 142(1):82–95, 1981. doi: 10.1086/337199. URL https://doi.org/10.1086/337199.

T. Fourcaud, F. Blaise, P. Lac, P. Castéra, and P. de Reffye. Numerical modelling of shape regulation and growth stresses in trees. *Trees*, 17(1):31–39, 2003. ISSN 1432-2285. URL https://doi.org/10.1007/s00468-002-0203-5.

M. Fournier, B. Chanson, D. Guitard, and B. Thibault. Mécanique de l'arbre sur pied : modélisation d'une structure en croissance soumise à des chargementspermanents et évolutifs. 1. analyse des contraintes de support. 1991a.

M. Fournier, B. Chanson, D. Guitard, and B. Thibault. Mécanique del'arbre sur pied :modélisation d'une structure en croissance soumise à des chargements permanents et évolutifs.2. analyse tridimensionnelle des contraintesde maturation, cas du feuillu standard. 1991b.

M. Fournier, H. Baillères, and B. Chanson. Tree biomechanics : growth, cumulative prestresses, and reorientations. *Biomimetics*, 2(3):229–251, 1994.

B. Ghislain, T. Alméras, J. Prunier, and B. Clair. Contributions of bark and tension wood and role of the g-layer lignification in the gravitropic movements of 21 tropical tree species. *Annals of Forest Science*, 76(4):107, 2019. ISSN 1297-966X. URL https://doi.org/10.1007/s13595-019-0899-7.

J. Gérard, D. Guibal, S. Paradis, M. Vernay, J. Beauchêne, L. Brancheriau, I. Châlon, C. Daigremont, P. Détienne, D. Fouquet, P. Langbour, S. Lotte, M.-F. Thévenon, C. Méjean, and A. Thibaut. Tropix 7, 2011. URL http://tropix.cirad.fr/en.

F. Hallé, R. A. Oldeman, and P. B. Tomlinson. *Tropical trees and forests: an architectural analysis*. Springer Verlag, 1978.

P. Heuret, C. Meredieu, T. Coudurier, F. Courdier, and D. Barthélémy. Ontogenetic trends in the morphological features of main stem annual shoots of pinus pinaster (pinaceae). *American Journal of Botany*, 93(11):1577–1587, 2006. doi: https://doi.org/10.3732/ajb.93.11.1577. URL https://bsapubs.onlinelibrary.wiley.com/doi/abs/10.3732/ajb.93.11.1577.

Y.-S. Huang, S.-S. Chen, L.-L. Kuo-Huang, and C.-M. Lee. Growth strain in the trunk and branches of chamaecyparis formosensis and its influence on tree form. *Tree Physiol*, 25(9):1119–1126, Sept. 2005. ISSN 0829-318X. URL https://doi.org/10.1093/treephys/25.9.1119.

Y.-S. Huang, L.-F. Hung, and L.-L. Kuo-Huang. Biomechanical modeling of gravitropic response of branches: roles of asymmetric periphery growth strain versus self-weight bending effect. *Trees*, 24(6):1151–1161, 2010. ISSN 1432-2285. URL https://doi.org/10.1007/s00468-010-0491-0.

L.-F. Hung, C.-C. Tsai, S.-J. Chen, Y.-S. Huang, and L.-L. Kuo-Huang. Study of tension wood in the artificially inclined seedlings of koelreuteria henryi dummer and its biomechanical function of negative gravitropism. *Trees*, 30(3):609–625, 2016. ISSN 1432-2285. URL https://doi.org/10.1007/s00468-015-1304-2.

L.-F. Hung, C.-C. Tsai, S.-J. Chen, Y.-S. Huang, and L.-L. Kuo-Huang. Strain distribution, growth eccentricity, and tension wood distribution in the plagiotropic and orthotropic branches of koelreuteria henryi dummer. *Trees*, 31(1):149–164, 2017. ISSN 1432-2285. URL https://doi.org/10.1007/s00468-016-1464-8.

L. J. Kucera and W. R. Philipson. Growth eccentricity and reaction anatomy in branchwood of drimys winteri and five native new zealand trees. *New Zealand Journal of Botany*, 15(3):517–524, 1977. doi: 10.1080/0028825X.1977.10429625. URL https://doi.org/10.1080/0028825X.1977.10429625.

H. Kübler. Studien über wachstumsspannungen des holzes iii. längenänderungen bei der wärmebehandlung frishen holzes. *Holz Rohst Werkst*, 17(3):77–86, 1959.

J. E. Nicholson. A rapid method for estimating longitudinal growth stresses in logs. *Wood Science and Technology*, 5(1):40–48, 1971. ISSN 1432-5225. URL https://doi.org/10.1007/BF00363119.

B. Thibaut. Three-dimensional printing, muscles, and skeleton: mechanical functions of living wood. *Journal of Experimental Botany*, 70(14):3453–3466, 04 2019. ISSN 0022-0957. doi: 10.1093/jxb/erz153. URL https://doi.org/10.1093/jxb/erz153.

B. Thibaut and J. Gril. Tree growth forces and wood properties. *Peer Community Journal*, 1:e46, 2021. doi: 10.24072/pcjournal.48. URL https://peercommunityjournal.org/articles/10.24072/pcjournal.48/.

T. E. Timell. *Compression wood in gymnosperms*, volume 1. Springer, 1986.

C.-C. Tsai, L.-F. Hung, C.-T. Chien, S.-J. Chen, Y.-S. Huang, and L.-L. Kuo-Huang. Biomechanical features of eccentric cambial growth and reaction wood formation in broadleaf tree branches. *Trees*, 26 (5):1585–1595, 2012. ISSN 1432-2285. URL https://doi.org/10.1007/s00468-012-0733-4.

Y. Wang, J. Gril, and J. Sugiyama. Variation in xylem formation of viburnum odoratissimum var. awabuki: growth strain and related anatomical features of branches exhibiting unusual eccentric growth. *Tree Physiol*, 29(5):707–713, May 2009a. ISSN 0829-318X. URL https://doi.org/10.1093/treephys/tpp007.

Y. Wang, J. Gril, and J. Sugiyama. Is the branch of viburnum odoratissimum var. awabuki reaction wood? unusual eccentric growth and various distributions of growth strain. In *6th Plant Biomechanics Conference*, pages 328–334, 2009b.

H. Yamamoto, M. Yoshida, and T. Okuyama. Growth stress controls negative gravitropism in woody plant stems. *Planta*, 216(2):280–292, 2002. ISSN 1432-2048. URL https://doi.org/10.1007/s00425-002-0846-x.

J. L. Yang, H. Baillères, T. Okuyama, A. Muneri, and G. Downes. Measurement methods for longitudinal surface strain in trees: a review. *Australian Forestry*, 68(1):34–43, 2005. doi: 10.1080/00049158.2005.10676224. URL https://doi.org/10.1080/00049158.2005.10676224.

M. Yoshida and T. Okuyama:. Techniques for measuring growth stress on the xylem surface using strain and dial gauges. 56(5):461–467, 2002. doi: doi:10.1515/HF.2002.071. URL https://doi.org/10.1515/HF.2002.071.

Appendix A

The calculation of integrals of the system 3 needs some preliminary elements. The situation of two consecutive rings is represented in figure 12. Each position x in the geometrical reference frame is expressed with respect to the position x' in the pith reference frame according to the equation:

$$x = r\cos\theta = x' - \overline{e}R \tag{24}$$

with r the radius at time t and R the radius at the final time.

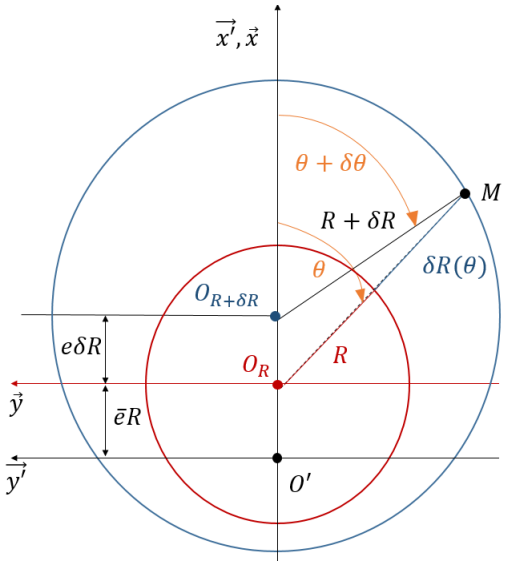

Figure 12: Representation of two consecutive rings and the elements needed to calculate $\delta R(\theta)$

Then, the integrals of the system 3 are computed as follows:

$$\begin{aligned}
\int_s \delta\sigma ds &= \int_s E\left[\delta a + (x + \overline{e}.R)\delta b\right] r\delta r d\theta \\
&= E\pi R^2\left(\delta a + \overline{e}.R\delta b\right) \\
\int_s x'\delta\sigma ds &= \int_s \left[\delta a + (x + \overline{e}.R)\delta b\right]\left[x + \overline{e}.R\right] r\delta r d\theta \\
&= E\pi R^3\left[\overline{e}\delta a + R\left(\overline{e}^2 + \frac{1}{4}\right)\delta b\right]
\end{aligned}$$

The tangential distribution of the radius increment $\delta R(\theta)$ are required in order to compute the terms of maturation. The Figure 12, enlighten that $\overrightarrow{OM} + \overrightarrow{MO'} = \overrightarrow{OO'}$:

$$\begin{cases}
\left[R + \delta R(\theta)\right]\cos\theta - (R + \delta R)\cos(\theta + \delta\theta) = e_R\delta R & \text{(25a)} \\
\left[R + \delta R(\theta)\right]\sin\theta - (R + \delta R)\sin(\theta + \delta\theta) = 0 & \text{(25b)}
\end{cases}$$

By setting $\delta\theta \to 0$, it comes:

$$\begin{cases}
\cos(\theta + \delta\theta) = \cos\theta - \sin\theta\delta\theta & \text{(26a)} \\
\sin(\theta + \delta\theta) = \sin\theta + \cos\theta\delta\theta & \text{(26b)}
\end{cases}$$

Substituting 26 into 25, and using the combination 25a.$\cos\theta$ + 25b.$\sin\theta$, $\delta R(\theta)$ can finally be written as:

$$\boxed{\delta R(\theta) = \delta R\left[1 + e_R \cos\theta\right]} \tag{27}$$

Then:

$$\begin{aligned}
\int_{\delta s} \sigma_0^i ds &= \int_{\delta s} \sigma_0^i(\theta) R\delta R(\theta) d\theta \\
&= \int_{\delta s} \left[\alpha + \beta\cos\theta\right]\left[1 + e\cos\theta\right] R\delta R(\theta) d\theta \\
&= \pi\left(2\alpha + e\beta\right) R\delta R \\
\int_{\delta s} x'\sigma_0^i ds &= \int_{\delta s} \sigma_0^i(\theta)(x + e.R) R\delta R(\theta) d\theta \\
&= R^2\delta R\pi\left(3\alpha e + \beta e^2 + \beta\right)
\end{aligned}$$

Appendix B

The matrix system 7 becomes:

$$\begin{cases}
\delta a = \dfrac{\delta F_0 K_2 - \delta F_1 K_1}{K_0 K_2 - K_1^2} & \text{(28a)} \\
\delta b = \dfrac{\delta F_0 K_1 - \delta F_1 K_0}{K_1^2 - K_0 K_2} & \text{(28b)}
\end{cases}$$

Then, numerators and denominators are calculated separately:

$$K_0 K_2 - K_1^2 = E^2\pi^2 R^6\left(\overline{e}^2 + \frac{1}{4}\right) - E^2\pi^2 R^6\overline{e}^2 = \frac{\left(E\pi R^3\right)^2}{4}$$

$$\begin{aligned}
\delta F_0 K_2 - \delta F_1 K_1 &= E\pi^2 R^5\left[-\left(2\alpha + e\beta\right)\left(\overline{e}^2 + \frac{1}{4}\right) + \overline{e}\left(3\alpha e + \beta e^2 + \beta\right)\right]\delta R + E\pi R^3\left[R\delta N\left(\overline{e}^2 + \frac{1}{4}\right) + \overline{e}\delta M\right] \\
&= E\pi^2 R^5\left[\alpha\left(3e\overline{e} - 2\overline{e}^2 - \frac{1}{2}\right) + \beta\left(\overline{e}e^2 - e\overline{e}^2 + \overline{e} - \frac{e}{4}\right)\right]\delta R + E\pi R^3\left[R\delta N\left(\overline{e}^2 + \frac{1}{4}\right) + \overline{e}\delta M\right]
\end{aligned}$$

$$\begin{aligned}
\delta F_0 K_1 - \delta F_1 K_0 &= E\pi^2 R^4\left[-\overline{e}\left(2\alpha + e\beta\right) + \left(3\alpha e + e^2\beta + \beta\right)\right]\delta R + E\pi R^2\left[\overline{e}R\delta N + \delta M\right] \\
&= E\pi^2 R^4\left[\alpha\left(3e - 2\overline{e}\right) + \beta\left(1 + e^2 - e\overline{e}\right)\right]\delta R + E\pi R^2\left[\overline{e}R\delta N + \delta M\right]
\end{aligned}$$

Putting the calculations together, system 28 becomes:

$$\begin{cases}
\delta a = \dfrac{4}{ER}\left[\alpha\left(3e\overline{e} - 2\overline{e}^2 - \dfrac{1}{2}\right) + \beta\left(\overline{e}e^2 - e\overline{e}^2 + \overline{e} - \dfrac{e}{4}\right)\right]\delta R + \dfrac{4}{E\pi R^3}\left[R\delta N\left(\overline{e}^2 + \dfrac{1}{4}\right) + \overline{e}\delta M\right] \\
\delta b = \dfrac{-4}{ER^2}\left[\alpha\left(3e - 2\overline{e}\right) + \beta\left(1 + e^2 - e\overline{e}\right)\right]\delta R + \dfrac{-4}{E\pi R^4}\left[\overline{e}R\delta N + \delta M\right]
\end{cases}$$

Appendix C

The following calculus is based on Figure 3.b). To get the vertical bending moment M_y of unit n (eq 23), one need the calculation of each volume V_n and center of gravity G_n. Lets fix $D(z)$ the deflection of the cone. It comes:

$$V_n = \int_0^{L_n} \frac{\pi D(z)^2}{4} dz \tag{30}$$

where $D(z) = D_n + \left(\frac{D_{n+1}-D_n}{L_n}\right) z$. One gives

$$O_n G_n = \frac{1}{V_n} \int_0^{L_n} \frac{\pi D(z)^2}{4} z dz \tag{31}$$

Setting $\gamma = \frac{D_{n+1}-D_n}{D_n}$ and $\xi = \frac{L_n}{z}$, the equation 30 and 31 then become:

$$V_n = \frac{\pi D_n^2 L_n}{4} \int_0^1 (1+\gamma\xi)^2 \, d\xi = \frac{\pi D_n^2 L_n}{4} . \left(1 + \gamma + \frac{\gamma^2}{3}\right)$$

$$O_n G_n = \frac{1}{V_n} \frac{\pi D_n^2 L_n^2}{4} . \left(\frac{1}{2} + \frac{2\gamma}{3} + \frac{\gamma^2}{4}\right)$$

So, finally, $O_n G_n$ can be written:

$$O_n G_n = \frac{L_n}{2} \left(\frac{1 + \frac{4}{3}\gamma + \frac{1}{2}\gamma^2}{1 + \gamma + \frac{1}{3}\gamma^2}\right) \tag{32}$$